

---

# GENERALIZED MOVING LEAST-SQUARES FOR SOLVING VECTOR-VALUED PDES ON UNKNOWN MANIFOLDS

---

A PREPRINT

**Rongji Li**

School of Information Science and Technology, ShanghaiTech University, Shanghai 201210, China  
lirj2022@shanghaitech.edu.cn

**Qile Yan**

School of Mathematics, University of Minnesota, 206 Church St SE, Minneapolis, MN 55455, USA  
yan00082@umn.edu

**Shixiao W. Jiang**

Institute of Mathematical Sciences, ShanghaiTech University, Shanghai 201210, China  
jiangshx@shanghaitech.edu.cn

June 19, 2024

## ABSTRACT

In this paper, we extend the Generalized Moving Least-Squares (GMLS) method in two different ways to solve the vector-valued PDEs on unknown smooth 2D manifolds without boundaries embedded in  $\mathbb{R}^3$ , identified with randomly sampled point cloud data. The two approaches are referred to as the intrinsic method and the extrinsic method. For the intrinsic method which relies on local approximations of metric tensors, we simplify the formula of Laplacians and covariant derivatives acting on vector fields at the base point by calculating them in a local Monge coordinate system. On the other hand, the extrinsic method formulates tangential derivatives on a submanifold as the projection of the directional derivative in the ambient Euclidean space onto the tangent space of the submanifold. One challenge of this method is that the discretization of vector Laplacians yields a matrix whose size relies on the ambient dimension. To overcome this issue, we reduce the dimension of vector Laplacian matrices by employing an appropriate projection. The complexity of both methods scales well with the dimension of manifolds rather than the ambient dimension. We also present supporting numerical examples, including eigenvalue problems, linear Poisson equations, and nonlinear Burgers' equations, to examine the numerical accuracy of proposed methods on various smooth manifolds.

**Keywords** Generalized Moving Least-Squares, Vector-valued PDEs, Unknown smooth manifolds, Randomly sampled point cloud data

# 1 Introduction

Solving vector-valued Partial Differential Equations (PDEs) on curved surfaces or embedded manifolds has various applications in natural sciences and practical engineering. Examples include transport processes of surfactants within thin films [23], surface dynamics of fluid vesicles and biomembranes [48, 4], formation of fractures and barriers on interfaces [35], tracking evolving geometries or even topological changes of interfaces [47], fluid flows in computer graphics [51], etc.

For such wide applications, there have been several developing numerical methods to approximate the solution of vector-valued PDEs on manifolds. Given a sufficient high-quality simplicial complex or mesh, both Discrete Exterior Calculus (DEC) [24, 10] and Finite Element Exterior Calculus (FEEC) [2, 25, 18] can achieve the desirable convergence in PDE problems for manifolds embedded in a low-dimensional ambient space. However, constructing meshes on surfaces with high quality can be difficult and complicated when the manifold is only identified by randomly sampled data.

To avoid this issue, various mesh-free approaches have been developed for solving PDEs in recent decades. For unknown manifolds with only a point cloud given, the first step of most mesh-free approaches is to characterize the manifolds using a parametrization scheme, such as local SVD methods [12, 60, 57], level set methods [6, 19, 59, 1], closest point methods [45, 41], orthogonal gradient methods [42], moving least squares [33], just to name a few. The second step is to approximate the differential operators acting on functions in the strong form along the tangent bundles using approaches including the Radial Basis Function (RBF) methods [15, 16], Generalized Moving Least-Squares (GMLS) [33, 20], Generalized Finite Difference Methods (GFDM) [54, 52]. In our previous work [22], the RBF method was extended to provide an accurate approximation of differential operators acting on vector fields of smooth manifolds. However, its effectiveness depends crucially on the choice of shape parameters in the radial basis function. Additionally, the computational cost of the method is high since the resulting discrete operators are dense matrices with their size dependent on the ambient dimension.

Alternatively, graph-based approaches, including Vector Diffusion Maps (VDM) [50] and Spectral Exterior Calculus (SEC) [5] can also be used as a mesh-free tool to approximate vector Laplacians for processing raw data in manifold learning applications. This type of approaches does not need a parametrization of a point cloud while restricted to approximate a certain type of differential operators.

In this paper, we consider solving vector-valued PDEs on two-dimensional unknown manifolds  $M$  without boundaries embedded in the Euclidean space  $\mathbb{R}^3$ , identified with randomly sampled point cloud data. Our goal here is to construct an approximation for differential operators acting on vector fields of smooth manifolds where the resulting matrices are sparse with size only dependent of the intrinsic dimension. Based on two different types of formulations of vector differential operators, we extend the GMLS methods in two different ways to approximate the vector differential operators and subsequently solve vector-valued PDEs on manifolds. The two approximations will be referred to as the intrinsic method and the extrinsic method.

For the intrinsic GMLS method, it in general involves with the local characterization of the Riemannian metric tensor and other geometric quantities of manifolds in local intrinsic coordinates [33, 20, 27]. In this paper, we derive the formula of the covariant derivative and Laplacians acting on vector fields at the base point in a local normal coordinate system. It turns out that the resulting formula can be much simplified by using the properties of the normal coordinate system so that it helps to reduce the computational cost in constructing the vector Laplacian matrices. Our derivations can be viewed as a generalization from the Laplace-Beltrami of functions in [33] to the covariant derivative and Laplacians of vector fields.

For the extrinsic GMLS method, the surface derivative in the local coordinate can be written as a projection of the appropriate derivative in the ambient space [53, 52, 26]. Then the extrinsic method relies on the discretization in the ambient space which can be computationally expensive for the vector case. In this paper, we apply an appropriate projection to reduce the size of vector Laplacian matrices from  $3N \times 3N$  to  $2N \times 2N$ , where  $N$  is the point cloud data size, 3 corresponds to the ambient dimension and 2 corresponds to the intrinsic dimension of manifolds. This dimension reduction can be numerically realized since all objects (e.g., functions and tensor fields) in this paper are confined to the tangent bundle of manifolds and the surfaces are all static without movement in the normal direction. In fact, this work improves the result in our previous work [22], saving the memory cost and computational cost especially when the ambient dimension  $n \sim 10 - 100$  is moderately large.

The paper is organized as follows. In Section 2, we provide a short review of the GMLS approach and its application in the approximation of tangent vectors on unknown manifolds identified by randomly sampled data points. In Section 3, we present the intrinsic formulation for approximating the Bochner Laplacian and the covariant derivative using GMLS. In Section 4, using the extrinsic formulation, we apply a projection technique to improve

the approximation for the Bochner Laplacian and the covariant derivative. In Section 5, we provide supporting numerical examples for solving vector-valued PDEs, particularly eigenvalue problems, Poisson equations, linear vector diffusion equations and nonlinear Burgers' equations. In Section 6, we conclude the paper with a summary and some open problems. We relegate the intrinsic approximation and extrinsic approximation of two other vector Laplacians to the Appendix A and Appendix B, respectively.

## 2 Preliminaries

### 2.1 Review of GMLS

The GMLS approach is a regression technique for approximating functions by a linear combination of local basis functions, such as local polynomials, based on a set of scattered data samples (see e.g. [40, 34, 32, 58, 37]). We now briefly review the application of GMLS approach on a 2D smooth manifold embedded in  $\mathbb{R}^3$ . Given a set of (distinct) nodes  $\mathbf{X}_M = \{\mathbf{x}_i\}_{i=1}^N \subset M$ . For a base point  $\mathbf{x}_0 \in \mathbf{X}_M \subset M$ , we denote its  $K$ -nearest neighbors in  $\mathbf{X}_M$  by  $S_{\mathbf{x}_0} = \{\mathbf{x}_{0,k}\}_{k=1}^K \subset \mathbf{X}_M$ . In most literature, such a set  $S_{\mathbf{x}_0}$  is called a "stencil". By definition, we have  $\mathbf{x}_{0,1} = \mathbf{x}_0$  to be the base point. We assume that the true tangent space of the manifold  $M$  is given at this moment. We will discuss the unknown manifold regime in the following subsection 2.2. Let  $T_{\mathbf{x}}M$  be the tangent space at point  $\mathbf{x} = (x^1, x^2, x^3) \in M$  and denote its orthonormal basis by  $\{\mathbf{t}_1(\mathbf{x}), \mathbf{t}_2(\mathbf{x})\}$ .

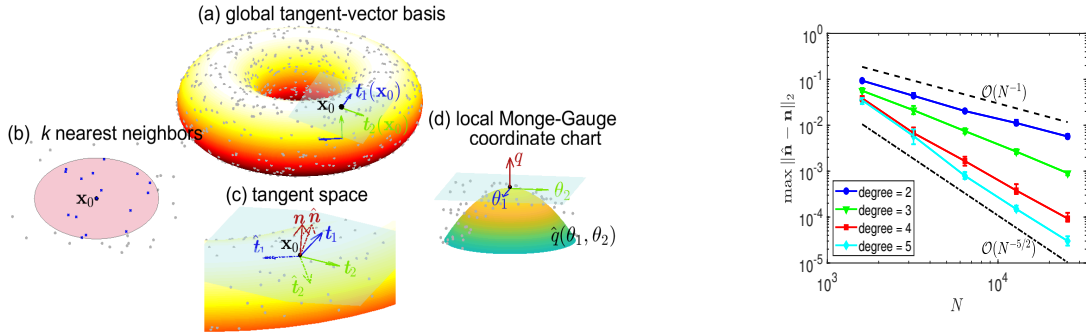


Figure 1: **Left panel:** Sketch of our setups. (a) Global tangent-vector bases  $\{\mathbf{t}_1, \mathbf{t}_2\}$  on the point cloud  $\{\mathbf{x}_i\}_{i=1}^N$  (gray dots) without alignment. (b)  $k$ -nearest neighbors of the base point  $\mathbf{x}_0$  plotted as blue crosses inside the red circle. (c) The tangent space  $\text{span}\{\mathbf{t}_1, \mathbf{t}_2\}$  and the normal  $\mathbf{n}$  at the base point  $\mathbf{x}_0$ . Also plotted are their estimations  $\{\hat{\mathbf{t}}_1, \hat{\mathbf{t}}_2, \hat{\mathbf{n}}\}$  given in (8) when the manifold is unknown. (d) The local Monge coordinate  $(\theta_1, \theta_2)$  and the GMLS approximation of the manifold  $\hat{q}(\theta_1, \theta_2)$  in the local coordinate chart (equation (9)). **Right panel:** Convergence results for the estimations of normal vectors on a torus, identified by randomly sampled data points.

The GMLS approach in this paper is formulated similarly as in [33, 20, 27, 26]. First, let  $\mathbb{P}_{\mathbf{x}_0}^l$  be the space of "intrinsic" polynomials with degree up to  $l$  in two variables at the base  $\mathbf{x}_0$ , i.e.,

$$\mathbb{P}_{\mathbf{x}_0}^l = \text{span}\{\theta_1^{\alpha_1} \theta_2^{\alpha_2} \mid 0 \leq |\alpha| \leq l\}, \quad (1)$$

where  $\theta_i(\mathbf{x}) = \mathbf{t}_i(\mathbf{x}_0) \cdot (\mathbf{x} - \mathbf{x}_0)$  ( $i = 1, 2$ ) are the local coordinates and  $\alpha = (\alpha_1, \alpha_2) \in \mathbb{N}^2$  is the multi-index notation with  $|\alpha| = \alpha_1 + \alpha_2$ . By definition, the dimension of the space  $\mathbb{P}_{\mathbf{x}_0}^l$  is  $m = (l+2)(l+1)/2$ . Given  $K > m$  and fitting data  $\mathbf{f}_{\mathbf{x}_0} = (f(\mathbf{x}_{0,1}), \dots, f(\mathbf{x}_{0,K}))^\top$ , we can define an operator  $\mathcal{S}_{\mathbb{P}} : \mathbf{f}_{\mathbf{x}_0} \in \mathbb{R}^K \rightarrow \mathcal{S}_{\mathbb{P}} \mathbf{f}_{\mathbf{x}_0} \in \mathbb{P}_{\mathbf{x}_0}^l$  such that  $\mathcal{S}_{\mathbb{P}} \mathbf{f}_{\mathbf{x}_0}$  is the optimal solution of the following moving least-squares problem:

$$\min_{\hat{f} \in \mathbb{P}_{\mathbf{x}_0}^l} \sum_{k=1}^K \lambda_k (f(\mathbf{x}_{0,k}) - \hat{f}(\mathbf{x}_{0,k}))^2, \quad (2)$$

where  $\lambda_k$  is some positive weight function. There are various choices of weighted  $\ell^2$ -norms in the moving least-squares (2) as shown in [58, 33, 20]. As reported in previous works [33, 26], the weight function

$$\lambda_k = \begin{cases} 1, & \text{if } k = 1, \\ 1/K, & \text{if } k = 2, \dots, K, \end{cases} \quad (3)$$

can numerically provide a stable approximation to the Laplace-Beltrami operator in many cases for randomly sampled nodes. Here we also apply such a special weight function for the stable vector Laplacians. For the covariant derivative, we choose the uniform weight function for a stable approximation.

The solution to the moving least-squares problem (2) can be represented as  $\hat{f}(\mathbf{x}) := (\mathcal{G}_{\mathbb{P}} \mathbf{f}_{\mathbf{x}_0})(\mathbf{x}) = \sum_{0 \leq \alpha_1 + \alpha_2 \leq l} b_{\alpha_1, \alpha_2} \theta_1^{\alpha_1}(\mathbf{x}) \theta_2^{\alpha_2}(\mathbf{x})$ , where the concatenated coefficients  $\mathbf{b} = (b_{\alpha(1)}, \dots, b_{\alpha(m)})^\top \in \mathbb{R}^{m \times 1}$  can be solved from a normal equation:

$$\mathbf{b} = (\Phi^\top \Lambda \Phi)^{-1} \Phi^\top \Lambda \mathbf{f}_{\mathbf{x}_0} := \Phi^\dagger \mathbf{f}_{\mathbf{x}_0}, \quad (4)$$

with  $\Lambda := \text{diag}(\lambda_1, \dots, \lambda_K) \in \mathbb{R}^{K \times K}$  and  $\Phi^\dagger := (\Phi^\top \Lambda \Phi)^{-1} \Phi^\top \Lambda \in \mathbb{R}^{m \times K}$ . Here  $\{\alpha(j)\}_{j=1}^m$  is the ordered multi-index  $\alpha(j) = (\alpha_1(j), \alpha_2(j))$  with  $0 \leq \alpha_1(j) + \alpha_2(j) \leq l$  for all  $j = 1, \dots, m$ . The above normal equation can be uniquely identified if  $\Phi = (\Phi_{kj}) \in \mathbb{R}^{K \times m}$  with

$$\Phi_{kj} = \theta_1^{\alpha_1(j)}(\mathbf{x}_{0,k}) \theta_2^{\alpha_2(j)}(\mathbf{x}_{0,k}), \quad 1 \leq k \leq K, 1 \leq j \leq m, \quad (5)$$

is a full rank matrix.

We now present the theoretical error estimates [37, 36] for such a GMLS approximation for partial derivative operators. For a set of points  $\mathbf{X}_M = \{\mathbf{x}_i\}_{i=1}^N \subset M$ , define the fill distance  $h_{\mathbf{X},M}$  and the separation distance  $q_{\mathbf{X},M}$  in Euclidean space as

$$h_{\mathbf{X},M} = \sup_{\mathbf{x} \in M} \min_{1 \leq j \leq N} \|\mathbf{x} - \mathbf{x}_j\|_2, \quad q_{\mathbf{X},M} = \frac{1}{2} \min_{i \neq j} \|\mathbf{x}_i - \mathbf{x}_j\|_2,$$

respectively, and assume that  $q_{\mathbf{X},M} \leq h_{\mathbf{X},M} \leq c_q q_{\mathbf{X},M}$  for some constant  $c_q > 0$ . Let  $\mathbf{X}_M \subseteq M$  be such that  $h_{\mathbf{X},M} \leq h_0$  for some constant  $h_0 > 0$  and  $M^* = \bigcup_{\mathbf{x} \in M} B(\mathbf{x}, C_2 h_0)$ , a union of geodesic ball over the length  $C_2 h_0$  with some constant  $C_2 > 0$ . Then for any  $f \in C^{l+1}(M^*)$  and  $\delta = (\delta_1, \delta_2)$  that satisfies  $|\delta| = \delta_1 + \delta_2 \leq l$ ,

$$|D^\delta f(\mathbf{x}) - \widehat{D^\delta f}(\mathbf{x})| \leq C h_{\mathbf{X},M}^{l+1-|\delta|} \max_{|\beta|=l+1} \|D^\beta f\|_{L^\infty(M^*)}, \quad (6)$$

for all  $\mathbf{x} \in M$  and some  $C > 0$  [37]. In the error bound above, we used the notation  $\widehat{D^\delta f}$  as the GMLS approximation to  $D^\delta f$  using local polynomials up to degree  $l$ , where  $D^\delta$  denotes a general multi-dimensional derivative with multi-index  $\delta$ . For uniformly i.i.d. random data  $\mathbf{X}_M \subseteq M$  on manifolds, with probability higher than  $1 - \frac{1}{N}$ , one can show that  $h_{\mathbf{X},M} = O((\log N/N)^{1/d})$ , where  $d$  is the intrinsic dimension [26]. In the case of a 2D manifold, we have that  $h_{\mathbf{X},M} = O(N^{-1/2})$  and consequently

$$|D^\delta f(\mathbf{x}) - \widehat{D^\delta f}(\mathbf{x})| = O(N^{-\frac{l+1-|\delta|}{2}}), \quad (7)$$

where we have ignored the log factor.

## 2.2 Approximation of tangent vectors for unknown manifolds

For the unknown manifold setup, we assume that we are only given a point cloud  $\{\mathbf{x}_i\}_{i=1}^N \subset M$  on the interior of the smooth manifold. To construct approximations of differential operators, we need to approximate bases of tangent vector space  $\{\mathbf{t}_1(\mathbf{x}), \mathbf{t}_2(\mathbf{x})\}$  on each point  $\{\mathbf{x}_i\}_{i=1}^N$ . We first use the local singular value decomposition (SVD) or local principal component analysis (PCA) for a coarse approximation of the tangent vectors [12, 60, 57, 33, 22]:

1. For each base point  $\mathbf{x}_0 \in \mathbb{R}^3$  and its  $K$ -nearest neighbors  $\{\mathbf{x}_{0,k}\}_{k=1}^K$ , construct the distance matrix  $\mathbf{D} := [\mathbf{D}_1, \dots, \mathbf{D}_K] \in \mathbb{R}^{3 \times K}$ , where  $\mathbf{D}_i = \mathbf{x}_{0,i} - \mathbf{x}_0$  ( $i = 1, \dots, K$ ).
2. Take a singular value decomposition of  $\mathbf{D} = \mathbf{V}_L \Sigma \mathbf{V}_R$ , and then obtain the leading 2-columns of  $\mathbf{V}_L \in \mathbb{R}^{3 \times 3}$ , denoted by  $\{\tilde{\mathbf{t}}_1(\mathbf{x}_0), \tilde{\mathbf{t}}_2(\mathbf{x}_0)\}$ , which approximates a tangent basis of  $T_{\mathbf{x}}M$ , as well as the last column of  $\mathbf{V}_L$ , denoted by  $\tilde{\mathbf{n}}(\mathbf{x}_0)$ , which approximates a normal vector (Fig. 1(c)).

Once the coarse approximation to the tangent vectors is obtained, one can apply the GMLS approach to get a more accurate approximation of the manifold as well as the tangent space [33, 20, 27]. In particular, one can construct a local coordinate system with the origin  $\mathbf{x}_0$  and the orthonormal basis  $\{\tilde{\mathbf{t}}_1, \tilde{\mathbf{t}}_2, \tilde{\mathbf{n}}\}$ . Then, a neighboring point  $\mathbf{x}$  around  $\mathbf{x}_0$  has the local coordinate  $(\tilde{\theta}_1, \tilde{\theta}_2, \tilde{q})$ , where  $\tilde{\theta}_i(\mathbf{x}) = \tilde{\mathbf{t}}_i(\mathbf{x}_0) \cdot (\mathbf{x} - \mathbf{x}_0)$  ( $i = 1, 2$ ) and  $\tilde{q}(\mathbf{x}) = \tilde{\mathbf{n}}(\mathbf{x}_0) \cdot (\mathbf{x} - \mathbf{x}_0)$ . An approximation of the manifold with higher accuracy could be calculated as follows:

3. Let  $\tilde{q}(\tilde{\theta}_1, \tilde{\theta}_2) = \sum_{0 \leq \alpha_1 + \alpha_2 \leq l} \tilde{a}_{\alpha_1, \alpha_2} \tilde{\theta}_1^{\alpha_1} \tilde{\theta}_2^{\alpha_2}$  be the optimal solution to the GMLS problem:

$$\min_{\tilde{q} \in \mathbb{P}_{\mathbf{x}_0}^l} \sum_{k=1}^K \lambda_k \left( \tilde{q}(\tilde{\theta}_1(\mathbf{x}_{0,k}), \tilde{\theta}_2(\mathbf{x}_{0,k})) - \tilde{q}(\mathbf{x}_{0,k}) \right)^2.$$

4. Solve the normal equation  $(\tilde{\Phi}^\top \Lambda \tilde{\Phi}) \tilde{\mathbf{a}} = \tilde{\Phi}^\top \Lambda \tilde{\mathbf{q}}_{\mathbf{x}_0}$  to obtain the concatenated regression coefficients  $\tilde{\mathbf{a}} = (\tilde{a}_{\alpha_1(j), \alpha_2(j)})_{\substack{j=1, \dots, m \\ 0 \leq \alpha_1 + \alpha_2 \leq l}} \in \mathbb{R}^{m \times 1}$ , where  $\tilde{\mathbf{q}}_{\mathbf{x}_0} = (\tilde{q}(\mathbf{x}_{0,1}), \dots, \tilde{q}(\mathbf{x}_{0,K}))^\top$  and  $\tilde{\Phi}$  is in the form of (5) but with  $\{\theta_1, \theta_2\}$  replaced by  $\{\tilde{\theta}_1, \tilde{\theta}_2\}$ . Thus, one arrives at the locally parametrized surface,  $\tilde{q}(\tilde{\theta}_1, \tilde{\theta}_2)$ .
5. The two tangent vectors are  $(1, 0, \partial_{\tilde{\theta}_1} \tilde{q})^\top$  and  $(0, 1, \partial_{\tilde{\theta}_2} \tilde{q})^\top$  in the local coordinate system with the basis  $\{\tilde{\mathbf{t}}_1, \tilde{\mathbf{t}}_2, \tilde{\mathbf{n}}\}$ . Then compute the two tangent vectors of  $\tilde{q}(\tilde{\theta}_1, \tilde{\theta}_2)$  at the base  $\mathbf{x}_0$  in the Cartesian coordinate system as:

$$\hat{\mathbf{t}}_k(\mathbf{x}_0) = \tilde{\mathbf{t}}_k(\mathbf{x}_0) + \frac{\partial \tilde{q}(0, 0)}{\partial \tilde{\theta}_k} \tilde{\mathbf{n}}(\mathbf{x}_0) = \begin{cases} \tilde{\mathbf{t}}_k(\mathbf{x}_0) + \tilde{a}_{1,0} \tilde{\mathbf{n}}(\mathbf{x}_0), & k = 1, \\ \tilde{\mathbf{t}}_k(\mathbf{x}_0) + \tilde{a}_{0,1} \tilde{\mathbf{n}}(\mathbf{x}_0), & k = 2. \end{cases} \quad (8)$$

6. Compute the normal vector  $\hat{\mathbf{n}} = \hat{\mathbf{t}}_1 \times \hat{\mathbf{t}}_2$  at  $\mathbf{x}_0$ . Repeat the above steps for each base point in  $\{\mathbf{x}_i\}_{i=1}^N$ .

In the right panel of Fig. 1, we numerically verify the convergence rate for the estimation of the normal vector  $\hat{\mathbf{n}}$  on a torus where the parametrization of the torus is defined as in (37). The points  $\{\mathbf{x}_i\}_{i=1}^N$  are randomly sampled with a uniform distribution in intrinsic coordinates. One can clearly see that the convergence rate is in good agreement with the above GMLS theoretical error bound of  $O(N^{-1/2})$  in (7) since the normal  $\hat{\mathbf{n}}$  and the two tangent  $\hat{\mathbf{t}}_1, \hat{\mathbf{t}}_2$  involve with the first-order derivative of the parametrized surface  $\tilde{q}(\tilde{\theta}_1, \tilde{\theta}_2)$ .

### 3 GMLS using intrinsic formulation

In this section, we approximate differential operators for vector fields using intrinsic formulation. In Section 3.1, we review GMLS for the local Monge patch parametrization of each stencil  $S_{\mathbf{x}_0}$  [27, 20]. In Section 3.2, we derive the numerical scheme to approximate the Bochner Laplacian acting on a vector field. Then we approximate the covariant derivative in Section 3.3. For readers not familiar with intrinsic differential geometry, please refer to Appendix A.1 for a short review.

#### 3.1 Monge parametrization

We first review the Monge parametrization [38, 43] for a two-dimensional manifold in  $\mathbb{R}^3$ , which has been used in [33, 27, 20] to approximate the local metric tensor and other local geometric quantities. Assume that we are given a true tangent vector basis  $\{\mathbf{t}_1(\mathbf{x}_0), \mathbf{t}_2(\mathbf{x}_0)\}$  for known manifolds (see Fig. 1(a)) or given the approximate tangent vector basis  $\{\hat{\mathbf{t}}_1(\mathbf{x}_0), \hat{\mathbf{t}}_2(\mathbf{x}_0)\}$  as in (8) for unknown manifolds (see Fig. 1(c)) at the base point  $\mathbf{x}_0$ . For the ease of discussion, we use  $\{\mathbf{t}_1(\mathbf{x}_0), \mathbf{t}_2(\mathbf{x}_0)\}$  to denote the tangent vector basis for both cases of known and unknown manifolds in this section. Thereafter one can obtain the normal vector  $\mathbf{n}(\mathbf{x}_0) = \mathbf{t}_1(\mathbf{x}_0) \times \mathbf{t}_2(\mathbf{x}_0)$ .

A local coordinate chart for the manifold near the base point could be defined using the embedding map  $q$ ,

$$q(\theta_1, \theta_2; \mathbf{x}_0) = \mathbf{x}_0 + \theta_1 \mathbf{t}_1(\mathbf{x}_0) + \theta_2 \mathbf{t}_2(\mathbf{x}_0) + q(\theta_1, \theta_2) \mathbf{n}(\mathbf{x}_0),$$

where  $(\theta_1, \theta_2)$  are local coordinates of  $\mathbf{x}$  as defined in (1) and  $q(\theta_1, \theta_2) = \mathbf{n}(\mathbf{x}_0) \cdot (\mathbf{x} - \mathbf{x}_0)$ . Here  $q$  is a smooth function over the  $(\theta_1, \theta_2)$ -plane which denotes the ‘‘height’’ of the manifold surface (see Fig. 1(d)). This is known as the Monge parametrization of manifold [38, 43].

Then the ‘‘height’’  $q$  is approximated as a polynomial function of the local coordinates  $(\theta_1, \theta_2)$  using the GMLS approach following the similar procedure introduced in Section 2.2. Here one key difference is the degrees of all ‘‘intrinsic’’ polynomials in the hypothesis space ranging from 2 to  $l$ , that is, the hypothesis space is  $\mathbb{P}_{\mathbf{x}_0}^l \setminus \mathbb{P}_{\mathbf{x}_0}^1 = \text{span}(\{\theta_1^{\alpha_1} \theta_2^{\alpha_2}\}_{2 \leq \alpha_1 + \alpha_2 \leq l})$ . Thus, the approximation of  $q$  is the optimal solution to the least-squares problem (2):

$$\hat{q} = \sum_{2 \leq \alpha_1 + \alpha_2 \leq l} a_{\alpha_1, \alpha_2} \theta_1^{\alpha_1} \theta_2^{\alpha_2}. \quad (9)$$

Note here that the constant term and two linear terms w.r.t.  $(\theta_1, \theta_2)$  are absent in  $\hat{q}$  (Fig. 1(d)) since the parameterized surface  $\hat{q}$  should pass through the base point  $\mathbf{x}_0$  and possess the tangent space  $T_{\mathbf{x}_0} M = \text{span}\{\mathbf{t}_1(\mathbf{x}_0), \mathbf{t}_2(\mathbf{x}_0)\}$ .

Observe that the coordinate representation for tangent vector bases in the vicinity of  $\mathbf{x}_0$  are  $(1, 0, \partial_{\theta_1} \hat{q})^\top$  and  $(0, 1, \partial_{\theta_2} \hat{q})^\top$  in the local basis  $\{\mathbf{t}_1, \mathbf{t}_2, \mathbf{n}\}$  (Fig. 1(d)). For  $\mathbf{x}$  close to  $\mathbf{x}_0$ , the tangent vector basis  $\{\mathbf{t}_1, \mathbf{t}_2\} \in T_{\mathbf{x}} M$  in the Cartesian coordinate system of ambient space  $\mathbb{R}^3$  are approximated as

$$\partial_k := \frac{\partial}{\partial \theta_k} = \mathbf{t}_k(\mathbf{x}_0) + \frac{\partial \hat{q}}{\partial \theta_k} \mathbf{n}(\mathbf{x}_0), \quad k = 1, 2. \quad (10)$$

The local Riemannian metric  $g = (g_{ij})_{i,j=1}^2$  for  $\mathbf{x} \in S_{\mathbf{x}_0}$  is approximated as

$$g = \begin{bmatrix} 1 + (\partial_{\theta_1} \hat{q})^2 & \partial_{\theta_1} \hat{q} \partial_{\theta_2} \hat{q} \\ \partial_{\theta_1} \hat{q} \partial_{\theta_2} \hat{q} & 1 + (\partial_{\theta_2} \hat{q})^2 \end{bmatrix}. \quad (11)$$

As usual, we use  $g^{ij}$  to denote the inverse metric tensor. Other geometric quantities can be similarly computed in the stencil  $S_{\mathbf{x}_0}$ .

### 3.2 Approximation of the Bochner Laplacian

For any vector field given on the point cloud  $\mathbf{X}_M$ , we write it as  $u = u^j \mathbf{t}_j$  where the components  $\{u^1, u^2\}$  are defined on the nodes  $\{\mathbf{x}_i\}_{i=1}^N$  and  $\{\mathbf{t}_1(\mathbf{x}_i), \mathbf{t}_2(\mathbf{x}_i)\}_{i=1}^N$  are bases of tangent vector space at each node. Note that there is no need to do alignments of these bases (as shown in Fig. 1(a)). To obtain a finite-difference type approximation of the Bochner Laplacian at a base point  $\mathbf{x}_0$ , we intend to find the weights  $\{\mathbf{w}^k \in \mathbb{R}^{2 \times 2}\}_{k=1}^K$  such that,

$$\Delta_B u(\mathbf{x}_0) \approx \sum_{k=1}^K \mathbf{w}^k u(\mathbf{x}_{0,k}) = (\mathbf{w}^1, \dots, \mathbf{w}^K) \mathbf{u}_{\mathbf{x}_0}, \quad (12)$$

where  $\{\mathbf{x}_{0,k}\}_{k=1}^K$  is the  $K$ -nearest neighbors of  $\mathbf{x}_0$ ,  $u(\mathbf{x}_{0,k}) = (u^1(\mathbf{x}_{0,k}), u^2(\mathbf{x}_{0,k}))^\top$  and  $\mathbf{u}_{\mathbf{x}_0} = (u^1(\mathbf{x}_{0,1}), u^2(\mathbf{x}_{0,1}), \dots, u^1(\mathbf{x}_{0,K}), u^2(\mathbf{x}_{0,K}))^\top \in \mathbb{R}^{2K \times 1}$ .

In Section 3.2.1, we derive the intrinsic formulation for the Bochner Laplacian in the local Monge coordinate system (10). In Section 3.2.2, we apply the GMLS to discretize the operator in the local Monge coordinate. Notice that the representation of vector fields in the local coordinate chart is different from that in the global  $\{\mathbf{t}_1, \mathbf{t}_2\}$ . In Section 3.2.3, we discuss how to obtain the weights in (12) and assemble these weights into a sparse  $2N \times 2N$  matrix where 2 corresponds to the intrinsic dimension of the surface.

#### 3.2.1 Approximation of geometric quantities in the local Monge coordinate

The computations for geometric quantities and function derivatives involved in the Bochner Laplacian  $\Delta_B u$  could be complicated. Fortunately, here we only focus on the values of  $\Delta_B u$  at the base point  $\mathbf{x}_0$  and their calculations can be much simplified by noticing that the Monge coordinate system as introduced in Section 3.1 is a normal coordinate system. In particular, we use the following properties of a normal coordinate system:

**Proposition 3.1.** *Let  $\{U_0; \xi^1, \dots, \xi^d\}$  be a normal coordinate system at  $\mathbf{x}_0$  where  $U_0 \subset M$  is an open neighborhood of  $\mathbf{x}_0$  and  $M$  is a  $d$ -dimensional manifold with Riemannian metric  $g$ . Denote the Christoffel symbol by  $\Gamma_{ij}^k$ . Then*

- (1) For all  $1 \leq i, j \leq d$ ,  $g_{ij}(\mathbf{x}_0) = \delta_{ij}$ .
- (2) For all  $1 \leq i, j, k \leq d$ ,  $\Gamma_{ij}^k(\mathbf{x}_0) = 0$ .
- (3) For all  $1 \leq i, j, k \leq d$ ,  $\partial_k g_{ij}(\mathbf{x}_0) = 0$ .

These properties can be easily verified by noticing that in the expression of the metric (11), the polynomial  $\hat{q}$  as defined in (9) has no constant term or linear terms w.r.t.  $\{\theta_1, \theta_2\}$ .

The Bochner laplacian acting on a vector field  $u = \tilde{u}^i \partial_i$  is defined as

$$\Delta_B u = g^{ij} \tilde{u}_{,ij}^k \partial_k,$$

where the components are computed by

$$\tilde{u}_{,ijk}^i = \frac{\partial \tilde{u}_{,j}^i}{\partial \theta_k} + \tilde{u}_{,j}^p \Gamma_{kp}^i - \tilde{u}_{,p}^i \Gamma_{kj}^p, \quad \tilde{u}_{,j}^i = \frac{\partial \tilde{u}^i}{\partial \theta_j} + \tilde{u}^k \Gamma_{jk}^i.$$

Applying Proposition 3.1 and noticing that the tangent plane bases in (10) are  $\partial_k|_{\mathbf{x}_0} = \mathbf{t}_k(\mathbf{x}_0)$ , one can simplify the Bochner Laplacian  $\Delta_B u(\mathbf{x}_0)$  as,

$$\begin{aligned} \Delta_B u(\mathbf{x}_0) &= g^{ij} \tilde{u}_{,ij}^k \partial_k|_{\mathbf{x}_0} = [(\tilde{u}_{,11}^1 + \tilde{u}_{,22}^1) \partial_1 + (\tilde{u}_{,11}^2 + \tilde{u}_{,22}^2) \partial_2] |_{\mathbf{x}_0}, \\ &= \{ [\partial_{11} \tilde{u}^1 + \partial_{22} \tilde{u}^1 + \tilde{u}^1 (\partial_1 \Gamma_{11}^1 + \partial_2 \Gamma_{12}^1) + \tilde{u}^2 (\partial_1 \Gamma_{21}^1 + \partial_2 \Gamma_{22}^1)] \mathbf{t}_1 \\ &\quad + [\tilde{u}^1 (\partial_1 \Gamma_{11}^2 + \partial_2 \Gamma_{12}^2) + \partial_{11} \tilde{u}^2 + \partial_{22} \tilde{u}^2 + \tilde{u}^2 (\partial_1 \Gamma_{21}^2 + \partial_2 \Gamma_{22}^2)] \mathbf{t}_2 \} |_{\mathbf{x}_0}, \end{aligned} \quad (13)$$

where we simplify the components  $\tilde{u}_{,jk}^i$  at  $\mathbf{x}_0$  using Proposition 3.1 as

$$\tilde{u}_{,jk}^i|_{\mathbf{x}_0} = \left( \frac{\partial \tilde{u}_{,j}^i}{\partial \theta_k} + \tilde{u}_{,j}^p \Gamma_{kp}^i - \tilde{u}_{,p}^i \Gamma_{kj}^p \right) \Big|_{\mathbf{x}_0} = \frac{\partial \tilde{u}_{,j}^i}{\partial \theta_k} \Big|_{\mathbf{x}_0} = \left( \frac{\partial^2 \tilde{u}^i}{\partial \theta_j \partial \theta_k} + \tilde{u}^m \frac{\partial \Gamma_{mj}^i}{\partial \theta_k} \right) \Big|_{\mathbf{x}_0}.$$

For the Christoffel symbol  $\Gamma_{kl}^i = \frac{1}{2} g^{im} \left( \frac{\partial g_{mk}}{\partial \theta_l} + \frac{\partial g_{ml}}{\partial \theta_k} - \frac{\partial g_{kl}}{\partial \theta_m} \right)$ , one can calculate its derivative at the base  $\mathbf{x}_0$  using Proposition 3.1 as

$$\frac{\partial \Gamma_{kl}^i}{\partial \theta_s} \Big|_{\mathbf{x}_0} = \frac{1}{2} g^{im} \left( \frac{\partial g_{mk}}{\partial \theta_s \partial \theta_l} + \frac{\partial g_{ml}}{\partial \theta_s \partial \theta_k} - \frac{\partial g_{kl}}{\partial \theta_s \partial \theta_m} \right) \Big|_{\mathbf{x}_0}.$$

Writing  $g_{ij}$  in terms of the function  $\hat{q}$  (see equation (11)), one can further simplify the derivative of the Christoffel symbol. For example, one can compute

$$\begin{aligned} \partial_1 \Gamma_{12}^1|_{\mathbf{x}_0} &= \frac{1}{2} g^{11} \left( \frac{\partial g_{11}}{\partial \theta_1 \partial \theta_2} + \frac{\partial g_{12}}{\partial \theta_1 \partial \theta_1} - \frac{\partial g_{12}}{\partial \theta_1 \partial \theta_1} \right) \Big|_{\mathbf{x}_0} = \frac{1}{2} \frac{\partial}{\partial \theta_2} \left( 2 \frac{\partial \hat{q}}{\partial \theta_1} \frac{\partial^2 \hat{q}}{\partial \theta_1 \partial \theta_1} \right) \Big|_{\mathbf{x}_0} \\ &= \left( \frac{\partial^2 \hat{q}}{\partial \theta_1 \partial \theta_2} \frac{\partial^2 \hat{q}}{\partial \theta_1 \partial \theta_1} \right) \Big|_{\mathbf{x}_0} = 2a_{2,0}a_{1,1}, \end{aligned} \quad (14)$$

where  $a_{\alpha_1, \alpha_2}$  are the coefficients of  $\hat{q}$  as in (9). Similarly, one can obtain all the derivatives of Christoffel symbols at  $\mathbf{x}_0$  for 2D manifolds:

$$\begin{aligned} \partial_1 \Gamma_{11}^1 &= 4(a_{2,0})^2, & \partial_2 \Gamma_{11}^1 &= 2a_{1,1}a_{2,0}, & \partial_1 \Gamma_{11}^2 &= 2a_{2,0}a_{1,1}, & \partial_2 \Gamma_{11}^2 &= 4a_{0,2}a_{2,0}, \\ \partial_1 \Gamma_{12}^1 &= 2a_{2,0}a_{1,1}, & \partial_2 \Gamma_{12}^1 &= (a_{1,1})^2, & \partial_1 \Gamma_{12}^2 &= (a_{1,1})^2, & \partial_2 \Gamma_{12}^2 &= 2a_{0,2}a_{1,1}, \\ \partial_1 \Gamma_{22}^1 &= 4a_{0,2}a_{2,0}, & \partial_2 \Gamma_{22}^1 &= 2a_{0,2}a_{1,1}, & \partial_1 \Gamma_{22}^2 &= 2a_{0,2}a_{1,1}, & \partial_2 \Gamma_{22}^2 &= 4(a_{0,2})^2, \end{aligned}$$

where the restriction notations  $|_{\mathbf{x}_0}$  are all omitted. Then one can calculate  $\Delta_B u(\mathbf{x}_0)$  in (13) as

$$\begin{aligned} \Delta_B u(\mathbf{x}_0) &= \left( \partial_{11} \tilde{u}^1 + \partial_{22} \tilde{u}^1 + \tilde{u}^1 \left[ 4(a_{2,0})^2 + (a_{1,1})^2 \right] + \tilde{u}^2 \left[ 2a_{2,0}a_{1,1} + 2a_{0,2}a_{1,1} \right] \right) \mathbf{t}_1(\mathbf{x}_0) \\ &+ \left( \tilde{u}^1 \left[ 2a_{2,0}a_{1,1} + 2a_{0,2}a_{1,1} \right] + \partial_{11} \tilde{u}^2 + \partial_{22} \tilde{u}^2 + \tilde{u}^2 \left[ 4(a_{0,2})^2 + (a_{1,1})^2 \right] \right) \mathbf{t}_2(\mathbf{x}_0). \end{aligned} \quad (15)$$

### 3.2.2 Approximation of function and its derivatives in the local Monge coordinate

Let  $u = \tilde{u}^i \partial_i$  be a vector field defined locally on the stencil  $S_{\mathbf{x}_0}$ , where  $\{\partial_1, \partial_2\}$  is the local basis defined in (10). Our goal here is to approximate the Bochner Laplacian  $\Delta_B$  acting on the vector field  $u$  at  $\mathbf{x}_0$  by a linear combination of the vector values on  $S_{\mathbf{x}_0}$ , i.e.,  $\{\tilde{u}(\mathbf{x}_{0,k}) = (\tilde{u}^1(\mathbf{x}_{0,k}), \tilde{u}^2(\mathbf{x}_{0,k}))^\top \in \mathbb{R}^{2 \times 1}\}_{k=1}^K$ . Thus, we are seeking the weights  $\{\tilde{\mathbf{w}}^k \in \mathbb{R}^{2 \times 2}\}_{k=1}^K$  such that,

$$\Delta_B u(\mathbf{x}_0) \approx \sum_{k=1}^K \tilde{\mathbf{w}}^k \tilde{u}(\mathbf{x}_{0,k}) = (\tilde{\mathbf{w}}^1, \dots, \tilde{\mathbf{w}}^K) \tilde{\mathbf{u}}_{\mathbf{x}_0} \in \mathbb{R}^{2 \times 1}, \quad (16)$$

where  $\tilde{\mathbf{u}}_{\mathbf{x}_0} := (\tilde{u}^1(\mathbf{x}_{0,1}), \tilde{u}^2(\mathbf{x}_{0,1}), \dots, \tilde{u}^1(\mathbf{x}_{0,K}), \tilde{u}^2(\mathbf{x}_{0,K}))^\top \in \mathbb{R}^{2K \times 1}$ .

The GMLS approximation of the vector field  $u = \tilde{u}^i \partial_i$  gives the GMLS solution to each component, i.e.,

$$\tilde{u}^1 = \sum_{0 \leq \alpha_1 + \alpha_2 \leq l} \beta_{\alpha_1, \alpha_2} \theta_1^{\alpha_1} \theta_2^{\alpha_2}, \quad \tilde{u}^2 = \sum_{0 \leq \alpha_1 + \alpha_2 \leq l} \gamma_{\alpha_1, \alpha_2} \theta_1^{\alpha_1} \theta_2^{\alpha_2}. \quad (17)$$

Then one can calculate the functions and their derivatives at  $\mathbf{x}_0$  as

$$\begin{aligned} \tilde{u}^1|_{\mathbf{x}_0} &= \beta_{0,0}, & \partial_{11} \tilde{u}^1|_{\mathbf{x}_0} &= 2\beta_{2,0}, & \partial_{22} \tilde{u}^1|_{\mathbf{x}_0} &= 2\beta_{0,2}, \\ \tilde{u}^2|_{\mathbf{x}_0} &= \gamma_{0,0}, & \partial_{11} \tilde{u}^2|_{\mathbf{x}_0} &= 2\gamma_{2,0}, & \partial_{22} \tilde{u}^2|_{\mathbf{x}_0} &= 2\gamma_{0,2}. \end{aligned}$$

Substituting all above into  $\Delta_B u(\mathbf{x}_0)$  in (15), one arrives at

$$\begin{aligned} \Delta_B u(\mathbf{x}_0) &= (\Delta_B u(\mathbf{x}_0))_1 \mathbf{t}_1(\mathbf{x}_0) + (\Delta_B u(\mathbf{x}_0))_2 \mathbf{t}_2(\mathbf{x}_0) \\ &= [2\beta_{2,0} + 2\beta_{0,2} + \beta_{0,0} (4(a_{2,0})^2 + (a_{1,1})^2) + \gamma_{0,0} (2a_{2,0}a_{1,1} + 2a_{0,2}a_{1,1})] \mathbf{t}_1(\mathbf{x}_0) \\ &+ [\beta_{0,0} (2a_{2,0}a_{1,1} + 2a_{0,2}a_{1,1}) + 2\gamma_{2,0} + 2\gamma_{0,2} + \gamma_{0,0} (4(a_{0,2})^2 + (a_{1,1})^2)] \mathbf{t}_2(\mathbf{x}_0) \\ &:= (\mathbf{A}_{11} \boldsymbol{\beta} + \mathbf{A}_{12} \boldsymbol{\gamma}) \mathbf{t}_1(\mathbf{x}_0) + (\mathbf{A}_{21} \boldsymbol{\beta} + \mathbf{A}_{22} \boldsymbol{\gamma}) \mathbf{t}_2(\mathbf{x}_0), \end{aligned} \quad (18)$$

where the first component of  $\Delta_B u(\mathbf{x}_0)$  is  $(\Delta_B u(\mathbf{x}_0))_1 := \mathbf{A}_{11} \boldsymbol{\beta} + \mathbf{A}_{12} \boldsymbol{\gamma}$  and the second component is  $(\Delta_B u(\mathbf{x}_0))_2 := \mathbf{A}_{21} \boldsymbol{\beta} + \mathbf{A}_{22} \boldsymbol{\gamma}$ . Here  $\boldsymbol{\beta} = (\beta_{\alpha_1(j), \alpha_2(j)})_{j=1}^m \in \mathbb{R}^{m \times 1}$  and  $\boldsymbol{\gamma} = (\gamma_{\alpha_1(j), \alpha_2(j)})_{j=1}^m \in \mathbb{R}^{m \times 1}$  are both  $m$  by 1 column vectors



and  $\{\mathbf{A}_{ij} \in \mathbb{R}^{1 \times m}\}_{i,j=1}^2$  are all 1 by  $m$  row vectors. Specifically,  $\mathbf{A}_{11}$  has three nonzero entries  $4(a_{2,0})^2 + (a_{1,1})^2, 2, 2$  corresponding to  $\beta_{0,0}, \beta_{2,0}, \beta_{0,2}$ , respectively, and  $\mathbf{A}_{12}$  has only one nonzero entry  $2a_{2,0}a_{1,1} + 2a_{0,2}a_{1,1}$  corresponding to  $\gamma_{0,0}$ .  $\mathbf{A}_{21}$  and  $\mathbf{A}_{22}$  are defined similarly.

We now look for the weights  $\{\tilde{\mathbf{w}}^k\}_{k=1}^K$  satisfying (16) using the above intrinsic formulation (18). Notice from (17) that the coefficients  $\boldsymbol{\beta}$  and  $\boldsymbol{\gamma}$  can be solved from normal equations by regressions  $\boldsymbol{\beta} = \Phi^\dagger \tilde{\mathbf{u}}_{\mathbf{x}_0}^1$  and  $\boldsymbol{\gamma} = \Phi^\dagger \tilde{\mathbf{u}}_{\mathbf{x}_0}^2$ , respectively, where  $\Phi^\dagger \in \mathbb{R}^{m \times K}$  is given in (4) and  $\tilde{\mathbf{u}}_{\mathbf{x}_0}^j = (\tilde{u}^j(\mathbf{x}_{0,1}), \dots, \tilde{u}^j(\mathbf{x}_{0,K}))^\top \in \mathbb{R}^{K \times 1}$  ( $j = 1, 2$ ). Then one can write  $(\Delta_B u(\mathbf{x}_0))_1$  as:

$$(\Delta_B u(\mathbf{x}_0))_1 = \mathbf{A}_{11} \Phi^\dagger \tilde{\mathbf{u}}_{\mathbf{x}_0}^1 + \mathbf{A}_{12} \Phi^\dagger \tilde{\mathbf{u}}_{\mathbf{x}_0}^2 := \tilde{\mathbf{w}}_{11}^* \tilde{\mathbf{u}}_{\mathbf{x}_0}^1 + \tilde{\mathbf{w}}_{12}^* \tilde{\mathbf{u}}_{\mathbf{x}_0}^2, \quad (19)$$

where  $\tilde{\mathbf{w}}_{11}^* = (\tilde{w}_{11}^1, \tilde{w}_{11}^2, \dots, \tilde{w}_{11}^K) \in \mathbb{R}^{1 \times K}$  and  $\tilde{\mathbf{w}}_{12}^* = (\tilde{w}_{12}^1, \tilde{w}_{12}^2, \dots, \tilde{w}_{12}^K) \in \mathbb{R}^{1 \times K}$  correspond to the first row of  $(\tilde{\mathbf{w}}^1, \dots, \tilde{\mathbf{w}}^K) \in \mathbb{R}^{2 \times 2K}$ . One can follow the same procedure to obtain the second row of  $(\tilde{\mathbf{w}}^1, \dots, \tilde{\mathbf{w}}^K)$ . Last one can stack all the components  $\{\tilde{w}_{ij}^k\}_{i,j=1,2}^{k=1, \dots, K}$  to form the weights  $(\tilde{\mathbf{w}}^1, \dots, \tilde{\mathbf{w}}^K) \in \mathbb{R}^{2 \times 2K}$  as desired in (16).

### 3.2.3 Matrix assembly of the Bochner Laplacian

In this section, we discuss how to calculate the weights  $\{\mathbf{w}^k\}$  in (12) from the weights  $\{\tilde{\mathbf{w}}^k\}$  and assemble all  $\{\mathbf{w}^k\}$  into the appropriate rows and columns of a sparse  $2N \times 2N$  Laplacian matrix  $\mathbf{L}_B$ . So far, we have obtained the components  $\{\tilde{u}(\mathbf{x}_{0,k}) \in \mathbb{R}^{2 \times 1}\}_{k=1}^K$  and the weights  $\{\tilde{\mathbf{w}}^k\}_{k=1}^K$  to approximate  $\Delta_B u(\mathbf{x}_0)$  (see equation (16)) in the local bases  $\{(\partial_1|_{\mathbf{x}_{0,k}}, \partial_2|_{\mathbf{x}_{0,k}})\}_{k=1}^K$  of each stencil  $S_{\mathbf{x}_0}$ . In order to construct a sparse  $2N \times 2N$  Bochner Laplacian matrix, we need to transform the weights from the local bases  $\{\partial_1|_{\mathbf{x}_{0,k}}, \partial_2|_{\mathbf{x}_{0,k}}\}_{k=1}^K$  in each  $S_{\mathbf{x}_0}$  to the unified global basis  $\{\mathbf{t}_1(\mathbf{x}_{0,k}), \mathbf{t}_2(\mathbf{x}_{0,k})\}_{k=1}^K$ .

Let  $\{\mathbf{w}^k\}_{k=1}^K$  be the weights as we seek in (12), then

$$\sum_{k=1}^K \mathbf{w}^k u(\mathbf{x}_{0,k}) = (\mathbf{w}^1, \dots, \mathbf{w}^K) \mathbf{u}_{\mathbf{x}_0} \approx \Delta_B u(\mathbf{x}_0) \approx \sum_{k=1}^K \tilde{\mathbf{w}}^k \tilde{u}(\mathbf{x}_{0,k}). \quad (20)$$

In particular, we let

$$\mathbf{w}^k u(\mathbf{x}_{0,k}) \approx \tilde{\mathbf{w}}^k \tilde{u}(\mathbf{x}_{0,k}), \quad \forall k = 1, \dots, K.$$

Besides, notice that  $u = u^j \mathbf{t}_j \approx \tilde{u}^i \partial_i$  in each  $S_{\mathbf{x}_0}$ , that is,

$$[\mathbf{t}_1(\mathbf{x}_{0,k}) \quad \mathbf{t}_2(\mathbf{x}_{0,k})] u(\mathbf{x}_{0,k}) \approx [\partial_1|_{\mathbf{x}_{0,k}} \quad \partial_2|_{\mathbf{x}_{0,k}}] \tilde{u}(\mathbf{x}_{0,k}) \in \mathbb{R}^{3 \times 1},$$

where  $\text{span}\{\partial_1, \partial_2\} \approx \text{span}\{\mathbf{t}_1, \mathbf{t}_2\}$  in the neighborhood of  $\mathbf{x}_0$  in which the small deviation is induced by the local approximation of Monge parametrization. In general, the bases  $\{\partial_1, \partial_2\}$  in (10) are not orthogonal at the neighboring  $\{\mathbf{x}_{0,k}\}_{k=2}^K$  due to nonflat geometry in the Taylor expansion,  $g_{ij}(\mathbf{x}_0) = \delta_{ij} + \sum_{k,l} \frac{1}{3} R_{iklj}(\mathbf{x}_0) \theta_k \theta_l + O(\|\theta\|^3)$ . Then we can solve the least-squares problem to obtain the weight  $\mathbf{w}^k$  for  $\forall k = 1, \dots, K$ :

$$\mathbf{w}^k \approx \tilde{\mathbf{w}}^k \left( \begin{bmatrix} \partial_1^\top|_{\mathbf{x}_{0,k}} \\ \partial_2^\top|_{\mathbf{x}_{0,k}} \end{bmatrix} \begin{bmatrix} \partial_1|_{\mathbf{x}_{0,k}} & \partial_2|_{\mathbf{x}_{0,k}} \end{bmatrix} \right)^{-1} \begin{bmatrix} \partial_1^\top|_{\mathbf{x}_{0,k}} \\ \partial_2^\top|_{\mathbf{x}_{0,k}} \end{bmatrix} [\mathbf{t}_1(\mathbf{x}_{0,k}) \quad \mathbf{t}_2(\mathbf{x}_{0,k})].$$

Then, we repeat the above procedure to obtain the weights for each point in  $\{\mathbf{x}_i\}_{i=1}^N$ . Last, we assemble all these weights  $\{\mathbf{w}^k\}$  into the appropriate rows and columns of a sparse  $2N \times 2N$  Laplacian matrix  $\mathbf{L}_B$  as a pointwise approximation to the Bochner Laplacian  $\Delta_B$  on the point cloud  $\{\mathbf{x}_i\}_{i=1}^N$ .

The complete procedure of the intrinsic GMLS approximation of the Bochner Laplacian is listed in Algorithm 1. Incidentally, one can follow the similar procedure to approximate other vector Laplacians acting on vector fields using the intrinsic method (See Appendix A).

### 3.3 Approximation of covariant derivative

Note that the covariant derivative of the vector field  $u = \tilde{u}^i \partial_i$  along itself could be written as

$$\nabla_u u = \tilde{u}_{;k}^i \tilde{u}^k \partial_i = \tilde{u}^k \left( \partial_k \tilde{u}^i + \tilde{u}^j \Gamma_{kj}^i \right) \partial_i.$$

By using the local Monge coordinate system introduced in Section 3.1, the approximation of  $\nabla_u u$  could be derived directly as

$$\begin{aligned} \nabla_u u(\mathbf{x}_0) &= \tilde{u}^k \left( \partial_k \tilde{u}^i + \tilde{u}^j \Gamma_{kj}^i \right) \partial_i \Big|_{\mathbf{x}_0} \\ &\approx (\beta_{0,0} \beta_{1,0} + \gamma_{0,0} \beta_{0,1}) \mathbf{t}_1(\mathbf{x}_0) + (\beta_{0,0} \gamma_{1,0} + \gamma_{0,0} \gamma_{0,1}) \mathbf{t}_2(\mathbf{x}_0), \end{aligned}$$

where the coefficients  $\beta_{\alpha_1, \alpha_2}$  and  $\gamma_{\alpha_1, \alpha_2}$  for  $0 \leq \alpha_1 + \alpha_2 \leq l$  are defined in (17). Here, we again use Proposition 3.1 to simplify the calculations.



**Algorithm 1** Intrinsic GMLS of the Bochner Laplacian

- 1: **Input:** A point cloud  $\{\mathbf{x}_i\}_{i=1}^N \subset M$ , bases of (estimated) tangent vector space at each node  $\{\mathbf{t}_1(\mathbf{x}_i), \mathbf{t}_2(\mathbf{x}_i)\}_{i=1}^N$ , the degree  $l$  of polynomials, and a parameter  $K > (l+2)(l+1)/2$  nearest neighbors.
- 2: Set  $\mathbf{L}_B$  to be a sparse  $2N \times 2N$  matrix with  $4NK$  nonzeros.
- 3: **for**  $i \in \{1, 2, \dots, N\}$  **do**
- 4: Find the  $K$  nearest neighbors of the point  $\mathbf{x}_i$  in the stencil  $S_{\mathbf{x}_i} = \{\mathbf{x}_{i,k}\}_{k=1}^K$ .
- 5: Find the GMLS approximation  $\hat{q}$  of the local embedding map as in (9).
- 6: Construct the local basis of  $\{\partial_1|_{\mathbf{x}_{i,k}}, \partial_2|_{\mathbf{x}_{i,k}}\}$  over the stencil  $S_{\mathbf{x}_i}$  as in (10).
- 7: Compute the geometric quantities in (15) using the coefficients of  $\hat{q}$ .
- 8: Calculate the weights  $\{\tilde{\mathbf{w}}^k\}_{k=1}^K$  using (19).
- 9: Calculate the weights  $\{\mathbf{w}^k\}_{k=1}^K$  as

$$\mathbf{w}^k = \tilde{\mathbf{w}}^k \left( \begin{bmatrix} \partial_1^\top|_{\mathbf{x}_{0,k}} \\ \partial_2^\top|_{\mathbf{x}_{0,k}} \end{bmatrix} \begin{bmatrix} \partial_1|_{\mathbf{x}_{0,k}} & \partial_2|_{\mathbf{x}_{0,k}} \end{bmatrix} \right)^{-1} \begin{bmatrix} \partial_1^\top|_{\mathbf{x}_{0,k}} \\ \partial_2^\top|_{\mathbf{x}_{0,k}} \end{bmatrix} \begin{bmatrix} \mathbf{t}_1(\mathbf{x}_{0,k}) & \mathbf{t}_2(\mathbf{x}_{0,k}) \end{bmatrix}.$$

- 10: Arrange the weights  $\{\mathbf{w}^k\}_{k=1}^K$  into corresponding rows and columns of  $\mathbf{L}_B$ .
- 11: **end for**
- 12: **Output:** The approximate operator matrix  $\mathbf{L}_B$ .

## 4 GMLS using extrinsic formulation

In this section, we approximate the operators on a point cloud using the extrinsic formulation. In Section 4.1, we review the representations of the differential operators on 2D surfaces as tangential derivatives [28, 17, 13, 49, 31, 22], which could be formulated as the projection of the appropriate derivatives in the ambient space. In Section 4.2, we approximate the extrinsic formulation of the gradient and the Bochner Laplacian of vector fields using the GMLS approach [33, 14, 20, 27, 26]. The vector fields here are represented using the bases from ambient space so that the resulting discrete Bochner Laplacian is of size  $3N \times 3N$  where  $N$  is the number of data points and 3 corresponds to the ambient dimension. In Section 4.3, we introduce a dimension reduction technique to convert the  $3N \times 3N$  matrix to a  $2N \times 2N$  matrix where 2 corresponds to the intrinsic dimension of the surface. In Section 4.4, we derive the formula for the approximation of covariant derivatives.

### 4.1 Review of extrinsic formulation of differential operators on manifolds

We first review some basic concepts and define the conventional notations in extrinsic differential geometry. For any point  $\mathbf{x} \in M$ , the local parametrization  $\iota: O \subset \mathbb{R}^2 \rightarrow M \subset \mathbb{R}^3$ , is defined through the following map,  $\Xi|_{\iota^{-1}(\mathbf{x})} \mapsto \mathbf{X}|_{\mathbf{x}}$ . Here,  $O$  denotes a open domain that contains the point  $\iota^{-1}(\mathbf{x})$ , which we denoted as  $\Xi_{\iota^{-1}(\mathbf{x})}$  in the canonical coordinates  $\left( \frac{\partial}{\partial \xi^1}, \frac{\partial}{\partial \xi^2} \right) \Big|_{\iota^{-1}(\mathbf{x})}$  and  $\mathbf{X}|_{\mathbf{x}}$  is the embedded point represented in the ambient coordinates  $\left( \frac{\partial}{\partial X^1}, \frac{\partial}{\partial X^2}, \frac{\partial}{\partial X^3} \right) \Big|_{\mathbf{x}}$ . The local coordinate  $(\xi^1, \xi^2)$  is chosen arbitrarily which can also be the same as the local Monge coordinate  $(\theta_1, \theta_2)$  in Section 3.1. The basic idea for the extrinsic formulation is to rewrite the surface derivatives in local  $(\xi^1, \xi^2)$  as the projection of the derivatives in the ambient space  $(X^1, X^2, X^3)$ .

Let  $T_{\mathbf{x}}M$  be the tangent space at point  $\mathbf{x} \in M$  and denote a set of orthonormal tangent-vector basis by  $\{\mathbf{t}_1(\mathbf{x}), \mathbf{t}_2(\mathbf{x})\}$ . Then the projection matrix  $\mathbf{P}$  which projects vectors in  $\mathbb{R}^3$  to  $T_{\mathbf{x}}M$  could be written as  $\mathbf{P} = \sum_{i=1}^2 \mathbf{t}_i \mathbf{t}_i^\top$  at any  $\mathbf{x} \in M$  (see e.g. [22] for more detailed properties about  $\mathbf{P}$ ). Subsequently, the surface gradient acting on a smooth function  $f: M \rightarrow \mathbb{R}$  evaluated at  $\mathbf{x} \in M$  in the Cartesian coordinates can be given by [28, 17, 13, 49, 31],

$$\text{grad}_g f(\mathbf{x}) = \overline{\text{grad}}_{\mathbb{R}^3} F(\mathbf{x}) = \left( \sum_{j=1}^2 \mathbf{t}_j \mathbf{t}_j^\top \right) \overline{\text{grad}}_{\mathbb{R}^3} F(\mathbf{x}), \quad (21)$$

where  $\overline{\text{grad}}_{\mathbb{R}^3} = [\partial_{X^1}, \partial_{X^2}, \partial_{X^3}]^\top$  is the usual gradient operator defined in  $\mathbb{R}^3$  and  $\text{grad}_g f := g^{ij} \frac{\partial f}{\partial \xi^i} \frac{\partial}{\partial \xi^j}$  is defined w.r.t. the Riemannian metric  $g$  induced by  $M$  from  $\mathbb{R}^3$ . Here,  $F$  is a smooth extension of  $f$  to an open subset in  $\mathbb{R}^3$  such that  $F|_M = f$ . Note that the identity (21) holds true since for any smooth function  $f \in C^\infty(M)$ , such an extension  $F$  exists and the identity does not depend on the chosen extension [30]. In the following, we will abuse the notation to use  $f$  as both a function defined on a surface and its extension to an open set in  $\mathbb{R}^3$ . Let  $\{\mathbf{e}_1, \mathbf{e}_2, \mathbf{e}_3\}$  be the standard orthonormal basis corresponding to the Cartesian coordinate  $\{X^1, X^2, X^3\}$  in  $\mathbb{R}^3$ . Then we can rewrite

(21) in component form as

$$\text{grad}_g f(\mathbf{x}) = \begin{bmatrix} (\mathbf{e}_1 \cdot \mathbf{P}) \cdot \overline{\text{grad}}_{\mathbb{R}^3} f(\mathbf{x}) \\ (\mathbf{e}_2 \cdot \mathbf{P}) \cdot \overline{\text{grad}}_{\mathbb{R}^3} f(\mathbf{x}) \\ (\mathbf{e}_3 \cdot \mathbf{P}) \cdot \overline{\text{grad}}_{\mathbb{R}^3} f(\mathbf{x}) \end{bmatrix} := \begin{bmatrix} \mathcal{G}_1 f(\mathbf{x}) \\ \mathcal{G}_2 f(\mathbf{x}) \\ \mathcal{G}_3 f(\mathbf{x}) \end{bmatrix}, \quad (22)$$

where  $\mathcal{G}_j = (\mathbf{e}_j \cdot \mathbf{P}) \cdot \overline{\text{grad}}_{\mathbb{R}^3}$  ( $j = 1, 2, 3$ ) is a differential operator.

In a nutshell, the basic idea of the extrinsic formulation for the covariant derivative follows from the definition of the tangential connection on a submanifold  $M$  of  $\mathbb{R}^n$  (see e.g. Example 4.9 of [30]). That is, for smooth vector fields  $u, y \in \mathfrak{X}(M)$ , the tangential connection can be defined as

$$\nabla_u y = \mathbf{P}(\bar{\nabla}_U Y|_M), \quad (23)$$

where  $\nabla$  is the Levi-Civita connection on  $M$ ,  $\bar{\nabla} : \mathfrak{X}(\mathbb{R}^n) \times \mathfrak{X}(\mathbb{R}^n) \rightarrow \mathfrak{X}(\mathbb{R}^n)$  is the Euclidean connection (directional derivative) on  $\mathbb{R}^n$  mapping  $(U, Y)$  to  $\bar{\nabla}_U Y$ ,  $\mathbf{P} : T\mathbb{R}^n \rightarrow TM$  is the orthogonal projection onto  $TM$ , and  $U$  and  $Y$  are extensions of  $u$  and  $y$  onto an open subset in  $\mathbb{R}^n$  such that  $U|_M = u$  and  $Y|_M = y$ , respectively. One can show that such extensions exist and the value is independent of the chosen extension and thus  $\nabla_u y$  is well defined. More details about geometry can also be found in [11, 39, 8, 3] and references therein.

We now review the extrinsic formulation in our previous work [22] for the gradient and the Bochner Laplacian of a 2D vector field when it has an extension in  $\mathbb{R}^3$ . For a vector  $u \in \mathfrak{X}(M)$ , its gradient in the local coordinate is defined to be a  $(2, 0)$  tensor field in  $\mathfrak{X}(M) \times \mathfrak{X}(M)$ ,  $\text{grad}_g u = \sharp \nabla u = g^{kj} \bar{u}^i_{;k} \frac{\partial}{\partial \xi^i} \otimes \frac{\partial}{\partial \xi^j}$ , where  $\sharp$  is the standard musical isomorphism notation to raise the index. Let  $U = U^k \frac{\partial}{\partial X^k}$  be a smooth extension of  $u = u^i \frac{\partial}{\partial \xi^i}$  to an open subset in  $\mathbb{R}^3$  satisfying  $U|_M = u$ . In fact,  $\{\frac{\partial}{\partial X^1}, \frac{\partial}{\partial X^2}, \frac{\partial}{\partial X^3}\} = \{\mathbf{e}_1, \mathbf{e}_2, \mathbf{e}_3\}$  is the standard orthonormal basis for the Cartesian coordinate system. Let  $U = (U^1, U^2, U^3)^\top \in \mathbb{R}^{3 \times 1}$  be the coordinate representation and let  $\frac{\partial}{\partial \mathbf{X}} = (\frac{\partial}{\partial X^1}, \frac{\partial}{\partial X^2}, \frac{\partial}{\partial X^3})^\top \in \mathbb{R}^{3 \times 1}$  be the gradient operator  $\overline{\text{grad}}_{\mathbb{R}^3}$ . Then one can obtain the extrinsic formulation for the gradient of a vector field (see e.g. [22, 21]):

$$\begin{aligned} \text{grad}_g u &= \mathbf{P}(\overline{\text{grad}}_{\mathbb{R}^3} U) \mathbf{P} = \mathbf{P} \frac{\partial U}{\partial \mathbf{X}} \mathbf{P} = \mathbf{P} \begin{bmatrix} \mathcal{G}_1 U^1 & \mathcal{G}_2 U^1 & \mathcal{G}_3 U^1 \\ \mathcal{G}_1 U^2 & \mathcal{G}_2 U^2 & \mathcal{G}_3 U^2 \\ \mathcal{G}_1 U^3 & \mathcal{G}_2 U^3 & \mathcal{G}_3 U^3 \end{bmatrix} \\ &:= (\mathcal{H}_1 U, \mathcal{H}_2 U, \mathcal{H}_3 U), \end{aligned} \quad (24)$$

where for any  $\mathbf{x} \in M$ , the projection matrix  $\mathbf{P} = [P_{ij}]_{i,j=1}^3$  is symmetric,  $\overline{\text{grad}}_{\mathbb{R}^n} U = \frac{\partial U}{\partial \mathbf{X}} = [\frac{\partial U^i}{\partial X^j}]_{i,j=1}^3$  is a  $3 \times 3$  matrix, and  $\mathcal{H}_s := \mathbf{P} \text{diag}(\mathcal{G}_s, \mathcal{G}_s, \mathcal{G}_s)$  has the form,

$$\mathcal{H}_s U := \mathbf{P} \begin{bmatrix} \mathcal{G}_s & & \\ & \mathcal{G}_s & \\ & & \mathcal{G}_s \end{bmatrix} \begin{bmatrix} U^1 \\ U^2 \\ U^3 \end{bmatrix} = \begin{bmatrix} P_{11} & P_{12} & P_{13} \\ P_{21} & P_{22} & P_{23} \\ P_{31} & P_{32} & P_{33} \end{bmatrix} \begin{bmatrix} \mathcal{G}_s & & \\ & \mathcal{G}_s & \\ & & \mathcal{G}_s \end{bmatrix} \begin{bmatrix} U^1 \\ U^2 \\ U^3 \end{bmatrix} \in \mathbb{R}^{3 \times 1}. \quad (25)$$

Using the above notations, one can eventually obtain the extrinsic formulation for the Bochner Laplacian acting on a vector field (see Section 2.6 of [22]),

$$\Delta_B u = g^{ij} u^k_{;ij} \frac{\partial}{\partial \xi^k} = \mathcal{H}_1 \mathcal{H}_1 U + \mathcal{H}_2 \mathcal{H}_2 U + \mathcal{H}_3 \mathcal{H}_3 U := \bar{\Delta}_B U. \quad (26)$$

Detailed derivations of the above formulation can be found in [22] or Appendix B.1.

## 4.2 Review of local approximation of differential operators on manifolds

We now apply the GMLS approach [33, 14, 53, 20, 26, 27] to approximate the Bochner Laplacian in (26). In order to approximate the differential operators  $\mathcal{H}_s$  in (25) and subsequently  $\bar{\Delta}_B$  in (26), we first briefly review the local GMLS approximation to the differential operator  $\mathcal{G}_s$  in (22) (see e.g. [26]).

For a smooth function  $f \in C^\infty(M)$ , let  $\mathbf{f}_{\mathbf{x}_0} = (f(\mathbf{x}_{0,1}), \dots, f(\mathbf{x}_{0,K}))^\top$  be the restriction of  $f$  on the stencil  $S_{\mathbf{x}_0} = \{\mathbf{x}_{0,k}\}_{k=1}^K$ . Using the GMLS approach as introduced in Section 2.1, we can approximate the differential operator  $\mathcal{G}_s$  as,

$$\mathcal{G}_s f(\mathbf{x}_{0,k}) \approx (\mathcal{G}_s \mathcal{I}_{\mathbb{P}} \mathbf{f}_{\mathbf{x}_0})(\mathbf{x}_{0,k}) = \sum_{0 \leq \alpha_1 + \alpha_2 \leq l} b_{\alpha_1, \alpha_2} \mathcal{G}_s \theta_1^{\alpha_1}(\mathbf{x}_{0,k}) \theta_2^{\alpha_2}(\mathbf{x}_{0,k}),$$

for any  $k = 1, \dots, K$  and  $s = 1, 2, 3$ , where  $\theta_i(\mathbf{x})$  ( $i = 1, 2$ ) are the local coordinates in (1) and  $b_{\alpha_1, \alpha_2}$  are the coefficients for  $(\mathcal{I}_P \mathbf{f}_{\mathbf{x}_0})(\mathbf{x}) = \sum b_{\alpha_1, \alpha_2} \theta_1^{\alpha_1}(\mathbf{x}) \theta_2^{\alpha_2}(\mathbf{x})$  as in (4). For each  $s = 1, 2, 3$ , the above relation can be written in matrix form as,

$$\begin{aligned} \begin{bmatrix} \mathcal{G}_s f(\mathbf{x}_{0,1}) \\ \vdots \\ \mathcal{G}_s f(\mathbf{x}_{0,K}) \end{bmatrix} &\approx \underbrace{\begin{bmatrix} (\mathcal{G}_s \theta_1^{\alpha_1(1)} \theta_2^{\alpha_2(1)})(\mathbf{x}_{0,1}) & \cdots & (\mathcal{G}_s \theta_1^{\alpha_1(m)} \theta_2^{\alpha_2(m)})(\mathbf{x}_{0,1}) \\ \vdots & \ddots & \vdots \\ (\mathcal{G}_s \theta_1^{\alpha_1(1)} \theta_2^{\alpha_2(1)})(\mathbf{x}_{0,K}) & \cdots & (\mathcal{G}_s \theta_1^{\alpha_1(m)} \theta_2^{\alpha_2(m)})(\mathbf{x}_{0,K}) \end{bmatrix}}_{\mathbf{B}_s} \underbrace{\begin{bmatrix} b_{\alpha(1)} \\ \vdots \\ b_{\alpha(m)} \end{bmatrix}}_{\mathbf{b}} \\ &= \mathbf{B}_s \Phi^\dagger \mathbf{f}_{\mathbf{x}_0} := \mathbf{G}_s \mathbf{f}_{\mathbf{x}_0}, \end{aligned} \quad (27)$$

where  $\mathbf{B}_s$  is a  $K$  by  $m$  matrix with  $[\mathbf{B}_s]_{ij} = (\mathcal{G}_s \theta_1^{\alpha_1(j)} \theta_2^{\alpha_2(j)})(\mathbf{x}_{0,i})$ ,  $\Phi^\dagger$  is a  $m$  by  $K$  matrix defined in (4) and  $\mathbf{G}_s = \mathbf{B}_s \Phi^\dagger$  is a  $K$  by  $K$  matrix for approximating  $\mathcal{G}_s$  locally in the stencil  $S_{\mathbf{x}_0}$ .

Let  $\mathbf{P}(\mathbf{x}_{0,k}) = [P_{ij}(\mathbf{x}_{0,k})]_{i,j=1}^3$  be the projection matrix at the point  $\mathbf{x}_{0,k}$ . Then we can define a tensor projection matrix  $\mathbf{P}^\otimes \in \mathbb{R}^{3K \times 3K}$  as

$$\begin{aligned} \mathbf{P}^\otimes &= \sum_{k=1}^K \mathbf{P}(\mathbf{x}_{0,k}) \otimes [\delta_{kk}]_{K \times K} = \sum_{k=1}^K \begin{bmatrix} P_{11}(\mathbf{x}_{0,k}) & P_{12}(\mathbf{x}_{0,k}) & P_{13}(\mathbf{x}_{0,k}) \\ P_{21}(\mathbf{x}_{0,k}) & P_{22}(\mathbf{x}_{0,k}) & P_{23}(\mathbf{x}_{0,k}) \\ P_{31}(\mathbf{x}_{0,k}) & P_{32}(\mathbf{x}_{0,k}) & P_{33}(\mathbf{x}_{0,k}) \end{bmatrix} \otimes [\delta_{kk}]_{K \times K} \\ &= \begin{bmatrix} \text{diag}(\mathbf{p}_{11}) & \text{diag}(\mathbf{p}_{12}) & \text{diag}(\mathbf{p}_{13}) \\ \text{diag}(\mathbf{p}_{21}) & \text{diag}(\mathbf{p}_{22}) & \text{diag}(\mathbf{p}_{23}) \\ \text{diag}(\mathbf{p}_{31}) & \text{diag}(\mathbf{p}_{32}) & \text{diag}(\mathbf{p}_{33}) \end{bmatrix}_{3K \times 3K}, \end{aligned} \quad (28)$$

where  $\otimes$  is the Kronecker product,  $\mathbf{p}_{ij} = (P_{ij}(\mathbf{x}_{0,1}), \dots, P_{ij}(\mathbf{x}_{0,K}))^\top \in \mathbb{R}^{K \times 1}$ , and  $\delta_{kk} \in \mathbb{R}^{K \times K}$  has only one nonzero value 1 in the  $k$ th row and  $k$ th column and has values 0 elsewhere. Note that  $\mathbf{P}^\otimes$  is a symmetric positive definite projection matrix that maps a vector field in  $\mathbb{R}^3$  onto the tangent space of  $M$  for the  $K$  neighboring points in  $S_{\mathbf{x}_0}$ .

Then the differential operator  $\mathcal{H}_s$  in (25) can be approximated as,

$$\mathbf{H}_s = \mathbf{P}^\otimes \begin{bmatrix} \mathbf{G}_s & & \\ & \mathbf{G}_s & \\ & & \mathbf{G}_s \end{bmatrix}_{3K \times 3K}, \quad (29)$$

and the Bochner Laplacian in (26) can be subsequently approximated in the stencil  $S_{\mathbf{x}_0}$  as,

$$\begin{aligned} \Delta_B u|_{S_{\mathbf{x}_0}} &= \bar{\Delta}_B U|_{S_{\mathbf{x}_0}} = \sum_{\ell=1}^3 \mathcal{H}_\ell \mathcal{H}_\ell U|_{S_{\mathbf{x}_0}} \approx \sum_{\ell=1}^3 \mathbf{H}_\ell \mathbf{H}_\ell \mathbf{U}_{\mathbf{x}_0} \\ &= \sum_{\ell=1}^3 \mathbf{P}^\otimes \begin{bmatrix} \mathbf{G}_\ell & & \\ & \mathbf{G}_\ell & \\ & & \mathbf{G}_\ell \end{bmatrix} \mathbf{P}^\otimes \begin{bmatrix} \mathbf{G}_\ell & & \\ & \mathbf{G}_\ell & \\ & & \mathbf{G}_\ell \end{bmatrix} \mathbf{P}^\otimes \mathbf{U}_{\mathbf{x}_0}, \end{aligned} \quad (30)$$

where  $\mathbf{U}_{\mathbf{x}_0} = ((\mathbf{U}_{\mathbf{x}_0}^1)^\top, (\mathbf{U}_{\mathbf{x}_0}^2)^\top, (\mathbf{U}_{\mathbf{x}_0}^3)^\top)^\top \in \mathbb{R}^{3K \times 1}$  with each component  $\mathbf{U}_{\mathbf{x}_0}^\ell = (U^\ell(\mathbf{x}_{0,1}), \dots, U^\ell(\mathbf{x}_{0,K}))^\top \in \mathbb{R}^{K \times 1}$  for  $\ell = 1, 2, 3$ , and  $\mathbf{U}_{\mathbf{x}_0} = \mathbf{P}^\otimes \mathbf{U}_{\mathbf{x}_0}$  since  $\mathbf{U}_{\mathbf{x}_0}$  always lives in the tangent bundle of  $M$ .

So far, we are following most procedures in our previous work [22], where the only difference is that now we use the GLMS regression approach, which yields a sparse Laplacian matrix, instead of a global RBF interpolation in [22], which yields a dense matrix. However, the discrete Bochner Laplacian matrix is still of size  $3N \times 3N$  which depends on the ambient dimension  $n = 3$  containing totally  $9NK$  nonzero entries. For other problems with small intrinsic dimension  $d$  and large ambient dimension  $n$ , the computation would be expensive for solving PDEs involving the Bochner Laplacian. In the next section, we introduce a dimension reduction technique to reduce the size of the Bochner Laplacian from  $3N \times 3N$  to  $2N \times 2N$  meanwhile reduce the number of nonzero entries from  $3^2 NK$  to  $2^2 NK$ , where 2 corresponds to the intrinsic dimension.

### 4.3 Reduction from ambient dimension to intrinsic dimension

For the dimension reduction, the key observation here is that the projection matrix has the decomposition as  $\mathbf{P}(\mathbf{x}) = \mathbf{T}(\mathbf{x})\mathbf{T}(\mathbf{x})^\top$  (see e.g. Proposition 2.1 of [22]) for any  $\mathbf{x} \in M$ , where  $\mathbf{T}(\mathbf{x}) = [\mathbf{t}_1(\mathbf{x}), \mathbf{t}_2(\mathbf{x})] \in \mathbb{R}^{3 \times 2}$  and  $\mathbf{t}_i(\mathbf{x}) = (t_{i,1}(\mathbf{x}), t_{i,2}(\mathbf{x}), t_{i,3}(\mathbf{x}))^\top \in \mathbb{R}^{3 \times 1}$  ( $i = 1, 2$ ) are the same global tangent vector basis used in Section 3.2. Then, the projection matrix  $\mathbf{P}^\otimes \in \mathbb{R}^{3K \times 3K}$  for  $K$  neighboring points in  $S_{\mathbf{x}_0}$  has the decomposition as  $\mathbf{P}^\otimes = \mathbf{T}^\otimes \mathbf{T}^{\otimes \top}$ , where  $\mathbf{T}^\otimes \in \mathbb{R}^{3K \times 2K}$  is given by

$$\mathbf{T}^\otimes = \sum_{k=1}^K [\mathbf{T}(\mathbf{x}_{0,k})]_{3 \times 2} \otimes [\delta_{kk}]_{K \times K} = \begin{bmatrix} \text{diag}(\mathbf{t}_{1,1}) & \text{diag}(\mathbf{t}_{2,1}) \\ \text{diag}(\mathbf{t}_{1,2}) & \text{diag}(\mathbf{t}_{2,2}) \\ \text{diag}(\mathbf{t}_{1,3}) & \text{diag}(\mathbf{t}_{2,3}) \end{bmatrix}. \quad (31)$$

Here,  $\delta_{kk}$  is defined as in (28) and  $\mathbf{t}_{i,j} = (t_{i,j}(\mathbf{x}_{0,1}), \dots, t_{i,j}(\mathbf{x}_{0,K}))^\top \in \mathbb{R}^{K \times 1}$  for  $i = 1, 2$  and  $j = 1, 2, 3$ . Then the Bochner Laplacian (30) in the stencil  $S_{\mathbf{x}_0}$  can be written as

$$\begin{aligned} \Delta_B u|_{S_{\mathbf{x}_0}} &\approx \sum_{\ell=1}^3 \mathbf{T}^\circ \left( \mathbf{T}^{\circ\top} \begin{bmatrix} \mathbf{G}_\ell & & \\ & \mathbf{G}_\ell & \\ & & \mathbf{G}_\ell \end{bmatrix} \mathbf{T}^\circ \right) \left( \mathbf{T}^{\circ\top} \begin{bmatrix} \mathbf{G}_\ell & & \\ & \mathbf{G}_\ell & \\ & & \mathbf{G}_\ell \end{bmatrix} \mathbf{T}^\circ \right) (\mathbf{T}^{\circ\top} \mathbf{U}_{\mathbf{x}_0}) \\ &:= \mathbf{T}^\circ \left( \sum_{\ell=1}^3 \mathbf{R}_\ell \mathbf{R}_\ell \right) (\mathbf{T}^{\circ\top} \mathbf{U}_{\mathbf{x}_0}). \end{aligned} \quad (32)$$

Here,  $\mathbf{R}_\ell := \mathbf{T}^{\circ\top} (\mathbf{I}_3 \otimes \mathbf{G}_\ell) \mathbf{T}^\circ \in \mathbb{R}^{2K \times 2K}$  with  $\mathbf{I}_3$  being a  $3 \times 3$  identity matrix,  $\mathbf{T}^{\circ\top} \mathbf{U}_{\mathbf{x}_0} \in \mathbb{R}^{2K \times 1}$  is the coordinate representation of the vector field  $u|_{S_{\mathbf{x}_0}}$  w.r.t. the global basis  $\{\mathbf{t}_j(\mathbf{x}_{0,k})\}_{j=1,2}^{k=1,\dots,K}$  and  $\sum_{\ell=1}^3 \mathbf{R}_\ell \mathbf{R}_\ell \in \mathbb{R}^{2K \times 2K}$  is the Bochner Laplacian matrix that maps  $u|_{S_{\mathbf{x}_0}}$  to  $(\Delta_B u)|_{S_{\mathbf{x}_0}}$  w.r.t. the global basis  $\{\mathbf{t}_j(\mathbf{x}_{0,k})\}$ .

In order to find the weights  $\{\mathbf{w}^k\}_{k=1}^K$  as in (12) to approximate  $\Delta_B u(\mathbf{x}_0)$ , we need to further analyze the structure of the differential matrix  $\mathbf{R}_\ell$ . From a geometric view point, the left multiplication of  $\mathbf{T}^{\circ\top}$  and the right multiplication of  $\mathbf{T}^\circ$  in the matrix  $\mathbf{R}_\ell = \mathbf{T}^{\circ\top} (\mathbf{I}_3 \otimes \mathbf{G}_\ell) \mathbf{T}^\circ$  correspond to the pointwise left projection and the pointwise right projection of the  $3K \times 3K$  matrix  $\mathbf{I}_3 \otimes \mathbf{G}_\ell$  onto the tangent spaces of  $\{\mathbf{x}_{0,k}\}_{k=1}^K$ . That is, the entries in the  $s^{\text{th}}$  and  $(K+s)^{\text{th}}$  rows of  $\mathbf{R}_\ell$  (w.r.t. the point  $\mathbf{x}_{0,s}$ ) and in the  $r^{\text{th}}$  and  $(K+r)^{\text{th}}$  columns (w.r.t. the point  $\mathbf{x}_{0,r}$ ) can be calculated by the following projection to form a  $2 \times 2$  block submatrix  $\hat{\mathbf{R}}_{sr}^\ell$ ,

$$\begin{aligned} \begin{bmatrix} \mathbf{t}_1(\mathbf{x}_{0,s})^\top \\ \mathbf{t}_2(\mathbf{x}_{0,s})^\top \end{bmatrix}_{2 \times 3} & \begin{bmatrix} (\mathbf{G}_\ell)_{sr} & 0 & 0 \\ 0 & (\mathbf{G}_\ell)_{sr} & 0 \\ 0 & 0 & (\mathbf{G}_\ell)_{sr} \end{bmatrix}_{3 \times 3} \begin{bmatrix} \mathbf{t}_1(\mathbf{x}_{0,r}) & \mathbf{t}_2(\mathbf{x}_{0,r}) \end{bmatrix}_{3 \times 2} \\ &= (\mathbf{G}_\ell)_{sr} \begin{bmatrix} \mathbf{t}_1(\mathbf{x}_{0,s})^\top \\ \mathbf{t}_2(\mathbf{x}_{0,s})^\top \end{bmatrix}_{2 \times 3} \begin{bmatrix} \mathbf{t}_1(\mathbf{x}_{0,r}) & \mathbf{t}_2(\mathbf{x}_{0,r}) \end{bmatrix}_{3 \times 2} := \hat{\mathbf{R}}_{sr}^\ell \in \mathbb{R}^{2 \times 2}, \end{aligned} \quad (33)$$

where  $(\mathbf{G}_\ell)_{sr}$  denotes the entry in the  $s^{\text{th}}$  row and  $r^{\text{th}}$  column of  $\mathbf{G}_\ell$ .

Using all these block submatrices  $\hat{\mathbf{R}}_{sr}^\ell$  for  $1 \leq s, r \leq K$  and  $\ell = 1, 2, 3$ , one can find the weights  $\{\mathbf{w}^k \in \mathbb{R}^{2 \times 2}\}_{k=1}^K$  satisfying  $\Delta_B u(\mathbf{x}_0) \approx \sum_{k=1}^K \mathbf{w}^k u(\mathbf{x}_{0,k})$  in (12) by

$$(\mathbf{w}^1, \dots, \mathbf{w}^K) = \sum_{\ell=1}^3 \left( \hat{\mathbf{R}}_{11}^\ell, \dots, \hat{\mathbf{R}}_{1K}^\ell \right) \begin{bmatrix} \hat{\mathbf{R}}_{11}^\ell \cdots \hat{\mathbf{R}}_{1K}^\ell \\ \vdots \quad \ddots \quad \vdots \\ \hat{\mathbf{R}}_{K1}^\ell \cdots \hat{\mathbf{R}}_{KK}^\ell \end{bmatrix} := \sum_{\ell=1}^3 (\hat{\mathbf{R}}_\ell \hat{\mathbf{R}}_\ell)_1, \quad (34)$$

where  $\hat{\mathbf{R}}_\ell$  is row and column equivalent to  $\mathbf{R}_\ell$ , that is,  $\hat{\mathbf{R}}_\ell$  can be obtained from  $\mathbf{R}_\ell$  in (32) by taking appropriate row and column interchanges. Here subscript-1 is to denote the elements in the first 2 rows of the enclosed  $2K \times 2K$  matrix  $\hat{\mathbf{R}}_\ell \hat{\mathbf{R}}_\ell$  corresponding to the Bochner Laplacian approximation at the base  $\mathbf{x}_0$ . Note that there is no need for a transformation of the weights here since only the global basis  $\{\mathbf{t}_1(\mathbf{x}_i), \mathbf{t}_2(\mathbf{x}_i)\}_{i=1}^N$  has been involved in the computation for the extrinsic formulation of the Bochner Laplacian. Following the above procedure, we can compute these weights for each base point  $\mathbf{x}_i$  ( $i = 1, \dots, N$ ) and then appropriately arrange them into a sparse  $2N$  by  $2N$  Bochner Laplacian matrix.

The complete procedure of the extrinsic GMLS approximation of the Bochner Laplacian is listed in Algorithm 2. See Section B.2 and Section B.3 for the extrinsic approximations of two other vector Laplacians acting on vector fields.

#### 4.4 Approximation of covariant derivative

We now compute the covariant derivative of a vector field  $u$  along itself at the base point  $\mathbf{x}_0$ ,  $\nabla_u u(\mathbf{x}_0)$ , in extrinsic formulation using the  $K$  neighboring points of  $\mathbf{x}_0$  in  $S_{\mathbf{x}_0}$ . Let  $U = (U^1, U^2, U^3)^\top$  be an extension of  $u = u^j \mathbf{t}_j$  so that  $(U^1, U^2, U^3)^\top = u^1 \mathbf{t}_1 + u^2 \mathbf{t}_2$ . The extrinsic formulation for the covariant derivative can be written as (see e.g. [22]),

$$\nabla_u u(\mathbf{x}_0) = \mathbf{P}(\tilde{\nabla}_U U)|_{\mathbf{x}_0} = \mathbf{T}\mathbf{T}^\top \begin{bmatrix} \frac{\partial U^1}{\partial X^1} & \frac{\partial U^1}{\partial X^2} & \frac{\partial U^1}{\partial X^3} \\ \frac{\partial U^2}{\partial X^1} & \frac{\partial U^2}{\partial X^2} & \frac{\partial U^2}{\partial X^3} \\ \frac{\partial U^3}{\partial X^1} & \frac{\partial U^3}{\partial X^2} & \frac{\partial U^3}{\partial X^3} \end{bmatrix} \begin{bmatrix} U^1 \\ U^2 \\ U^3 \end{bmatrix} \Big|_{\mathbf{x}_0}, \quad (35)$$

where  $\mathbf{T} = [\mathbf{t}_1, \mathbf{t}_2] \in \mathbb{R}^{3 \times 2}$  is the global tangent vector basis. Then we approximate  $\left[ \frac{\partial U^r}{\partial X^s} \right]_{r,s=1}^3$  using GMLS approach. Notice that  $\frac{\partial}{\partial X^s} = (\mathbf{e}_s \cdot \mathbf{I}) \cdot \overline{\text{grad}}_{\mathbb{R}^3}$  can be obtained from  $\mathcal{G}_s = (\mathbf{e}_s \cdot \mathbf{P}) \cdot \overline{\text{grad}}_{\mathbb{R}^3}$  in (22) by replacing the projection  $\mathbf{P}$

**Algorithm 2** Extrinsic GMLS of the Bochner Laplacian

- 
- 1: **Input:** A point cloud  $\{\mathbf{x}_i\}_{i=1}^N \subset M$ , bases of (estimated) tangent vector space at each node  $\{\mathbf{t}_1(\mathbf{x}_i), \mathbf{t}_2(\mathbf{x}_i)\}_{i=1}^N$ , (estimated) projection matrices  $\mathbf{P}$ , the degree  $l$  of polynomials, and a parameter  $K > (l+2)(l+1)/2$  nearest neighbors.
  - 2: Set  $\mathbf{L}_B$  to be a sparse  $2N \times 2N$  matrix with  $4NK$  nonzeros.
  - 3: **for**  $i \in \{1, 2, \dots, N\}$  **do**
  - 4: Find the  $K$  nearest neighbors of the point  $\mathbf{x}_i$  in the stencil  $S_{\mathbf{x}_i} = \{\mathbf{x}_{i,k}\}_{k=1}^K$ .
  - 5: Construct the differential matrix  $\mathbf{G}_\ell$  as in (27).
  - 6: Calculate the block submatrices  $\hat{\mathbf{R}}_{sr}^\ell$  as in (33) for  $1 \leq s, r \leq K, \ell = 1, 2, 3$ .
  - 7: Find the weights  $\{\mathbf{w}^k\}_{k=1}^K$  as in (34).
  - 8: Arrange the weights  $\{\mathbf{w}^k\}_{k=1}^K$  into corresponding rows and columns of  $\mathbf{L}_B$ .
  - 9: **end for**
  - 10: **Output:** The approximate operator matrix  $\mathbf{L}_B$ .
- 

with the identity  $\mathbf{I}$ . Following the similar formula as in (27), one can construct a  $K$  by  $K$  differential matrix  $\mathbf{D}_s$  to approximate  $\frac{\partial}{\partial X^s}$  in  $S_{\mathbf{x}_0}$ . Taking the first row of  $\mathbf{D}_s$ , denoted by  $\mathbf{D}_{s1} \in \mathbb{R}^{1 \times K}$ , one can approximate the value of  $\frac{\partial U^r}{\partial X^s}|_{\mathbf{x}_0}$  as  $\mathbf{D}_{s1} \mathbf{U}_{\mathbf{x}_0}^r$  for  $1 \leq r, s \leq 3$ , where  $\mathbf{U}_{\mathbf{x}_0}^r = (U^r(\mathbf{x}_{0,1}), \dots, U^r(\mathbf{x}_{0,K}))^\top \in \mathbb{R}^{K \times 1}$  has been defined right after (30). Then the covariant derivative (35) can be calculated as

$$\begin{aligned} \nabla_u u(\mathbf{x}_0) &= \mathbf{T}(\mathbf{x}_0) \mathbf{T}(\mathbf{x}_0)^\top \begin{bmatrix} \mathbf{D}_{11} \mathbf{U}_{\mathbf{x}_0}^1 & \mathbf{D}_{21} \mathbf{U}_{\mathbf{x}_0}^1 & \mathbf{D}_{31} \mathbf{U}_{\mathbf{x}_0}^1 \\ \mathbf{D}_{11} \mathbf{U}_{\mathbf{x}_0}^2 & \mathbf{D}_{21} \mathbf{U}_{\mathbf{x}_0}^2 & \mathbf{D}_{31} \mathbf{U}_{\mathbf{x}_0}^2 \\ \mathbf{D}_{11} \mathbf{U}_{\mathbf{x}_0}^3 & \mathbf{D}_{21} \mathbf{U}_{\mathbf{x}_0}^3 & \mathbf{D}_{31} \mathbf{U}_{\mathbf{x}_0}^3 \end{bmatrix} \begin{bmatrix} U^1(\mathbf{x}_0) \\ U^2(\mathbf{x}_0) \\ U^3(\mathbf{x}_0) \end{bmatrix} \\ &= \mathbf{T}(\mathbf{x}_0) \mathbf{T}(\mathbf{x}_0)^\top \begin{bmatrix} (\mathbf{U}_{\mathbf{x}_0}^1)^\top \\ (\mathbf{U}_{\mathbf{x}_0}^2)^\top \\ (\mathbf{U}_{\mathbf{x}_0}^3)^\top \end{bmatrix}_{3 \times K} [\mathbf{D}_{11}^\top \quad \mathbf{D}_{21}^\top \quad \mathbf{D}_{31}^\top]_{K \times 3} \begin{bmatrix} U^1(\mathbf{x}_0) \\ U^2(\mathbf{x}_0) \\ U^3(\mathbf{x}_0) \end{bmatrix}. \end{aligned}$$

## 5 Numerical results

In this section, we show supporting numerical examples, including eigenvalue problems, Poisson equations, linear vector diffusion equations and nonlinear Burgers' equations. In Section 5.1 we numerically investigate the eigenvalue stability of the Bochner Laplacian on manifolds. In Section 5.2, we verify the numerical convergence of the Bochner Laplacian for solving Poisson equations. In Section 5.3 and Section 5.4, we study the numerical performance of the linear vector diffusion equation and the nonlinear viscous Burgers' equation, respectively.

In our numerical implementation, we only consider the regime of unknown manifolds, that is, we are only given a point cloud on unknown smooth manifolds. We apply the algorithm outlined in Section 2.2 to approximate the tangent space of the manifolds without alignment as shown in Fig. 1. For time-independent problems, we choose the polynomial degree of manifolds in GMLS to be identical to that used for functions. For time-dependent problems, the degree of manifolds is chosen to be 6 which is higher than that used for functions ( $l = 2, 3, 4, 5$ ) such that the error from manifold approximation is negligible. Besides, the parameter  $K$  in  $K$ -nearest neighbors are taken large enough, typically around 51 ~ 71, to yield a stable approximation of the Bochner Laplacian. The following numerical experiments demonstrate that the GMLS approaches can provide stable estimators and convergent results with small error bars, given various trials of independent randomly sampled data points.

### 5.1 Eigenvalue stability

In this subsection, we investigate the eigenvalue problem of the Bochner Laplacian on two examples. For PDE applications, a necessary condition for stability is that all eigenvalues of the discrete vector Laplacian have negative real parts. The first example is a 1D ellipse in  $\mathbb{R}^2$  with the parameterization,  $\mathbf{x} = (\cos\theta, 2\sin\theta)$ , where  $0 \leq \theta < 2\pi$ . For a 1D manifold, the Bochner Laplacian shares the same eigenvalues as the Hodge Laplacian, as well as the Laplace-Beltrami (see e.g., [22]). Here, the true eigenvalues can be approximated semi-analytically by solving the Sturm-Liouville form of the Laplace-Beltrami operator using the finite difference method (see p. 68 of [44]). The second example is a 2D unit sphere embedded in  $\mathbb{R}^3$ . We notice that the eigenvalues of the Bochner Laplacian are different from those of the Hodge Laplacian by a constant Ricci curvature on a unit sphere, where the non-trivial eigenvalues of the Hodge Laplacian are identical with the non-trivial eigenvalues of the Laplace-Beltrami operator

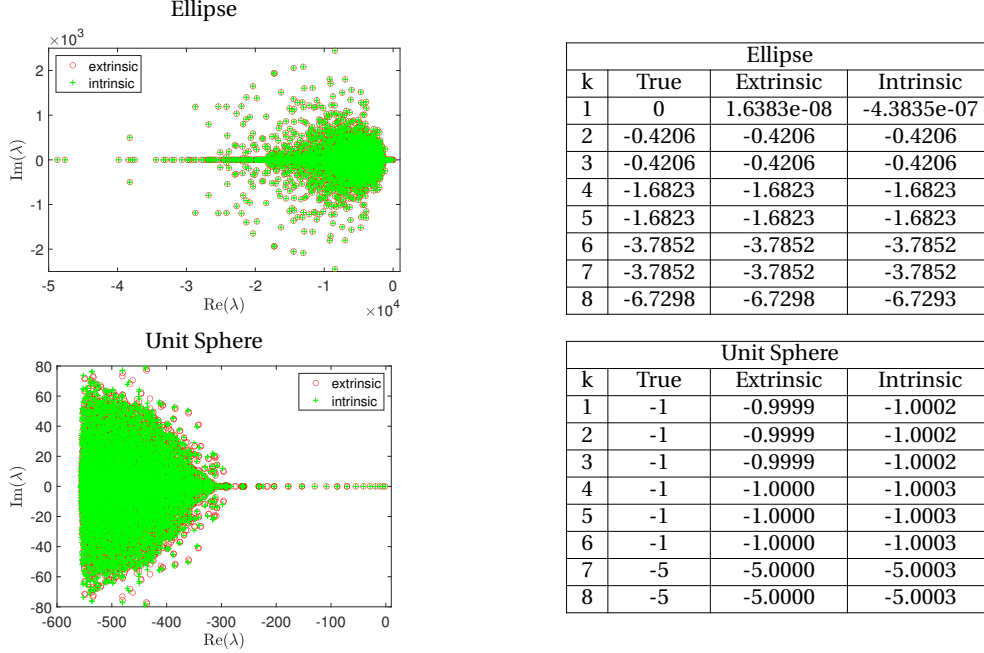


Figure 2: **Eigenvalues on 1D ellipse in  $\mathbb{R}^2$  and 2D sphere in  $\mathbb{R}^3$ .** In both examples,  $K = 51$ ,  $l = 5$ , and  $N = 6400$  points are randomly sampled. The first column: all eigenvalues lie in the left half complex plane. The second column: comparison of the leading 8 eigenvalues of the Bochner Laplacian between our approximation using intrinsic and extrinsic methods and the semi-analytic true solution.

but with double multiplicities (see e.g., [22]). In our numerical implementation, data points  $\{\mathbf{x}_i\}_{i=1}^N$  are randomly sampled with a uniform distribution in intrinsic coordinates on these two manifolds.

In the first column of Fig. 2, we plot all the eigenvalues of the non-symmetric Bochner Laplacian matrices in the complex plane. We see that all the eigenvalues lie in the left half complex plane with non-positive real parts to achieve the eigenvalue stability of the GMLS approximation. In the second column of Fig. 2, we further observe that the leading 8 numerical eigenvalues are in good agreement with the semi-analytic true eigenvalues. However, when there is a zero eigenvalue, the GMLS approximation possibly provides only one corresponding value which is slightly greater than zero and all the other eigenvalues having strictly negative real parts (see  $\hat{\lambda}_0 = 1.6e-8$  in the ellipse example, where  $\hat{\lambda}_0$  is a numerical eigenvalue with a positive real part close to zero.) In the following PDE applications, we always first test the eigenvalue stability before solving the PDE problems. If there is a numerical eigenvalue having small positive real part as in the ellipse example, we will regularize the Bochner Laplacian matrix by subtracting a constant from its diagonal entries,  $L_B - \hat{\lambda}_0 \mathbf{I}$ , to guarantee the eigenvalue stability where  $\mathbf{I}$  is an identity matrix.

## 5.2 Poisson problems

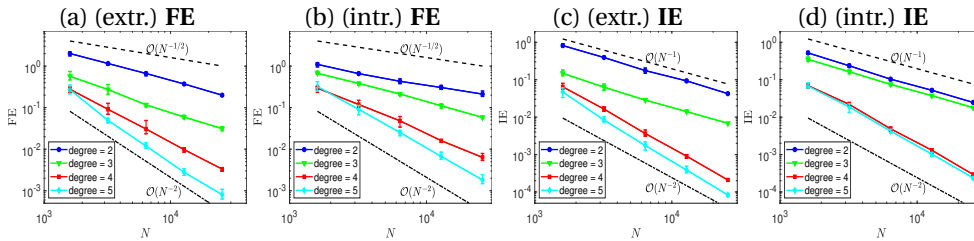


Figure 3: **Poisson problems on 2D torus in  $\mathbb{R}^3$ .** Random data with 6 trials.  $K = 51$  nearest neighbors are used. In panels (a) and (b), shown are the average FEs of the approximate Bochner Laplacian  $L_B$  using extrinsic and intrinsic methods, respectively. In panels (c) and (d), shown are the average IEs of the solutions of the Poisson problem (36).



In this subsection, we consider solving the following vector-valued Poisson problem for  $u \in \mathfrak{X}(M)$ ,

$$(a - \Delta_B)u = f, \quad \mathbf{x} \in M, \quad (36)$$

where  $a = 1 > 0$  and  $f \in \mathfrak{X}(M)$  are defined such that the problems are well-posed. Here, we notice that the vector fields  $f$  and  $u$  must live in the tangent bundle  $TM$  of the smooth manifold  $M$ . For the setup of an unknown manifold,  $f$  is replaced by  $\hat{\mathbf{T}}^\top F$  in our numerical implementation where  $\hat{\mathbf{T}} = [\hat{\mathbf{t}}_1, \hat{\mathbf{t}}_2]$  corresponds to the approximate tangent vectors and  $F \in \mathfrak{X}(\mathbb{R}^3)$  is a vector field in ambient space. Thus, the vector field  $\hat{\mathbf{T}}^\top F$  and the approximate solution  $\hat{u} = (a - \mathbf{L}_B)^{-1}(\hat{\mathbf{T}}^\top F)$  both live in the approximate tangent bundle  $\widehat{TM} := \cup_{\mathbf{x} \in M} \widehat{T}_{\mathbf{x}}M = \cup_{\mathbf{x} \in M} \text{Span}\{\hat{\mathbf{t}}_1(\mathbf{x}), \hat{\mathbf{t}}_2(\mathbf{x})\}$ .

In this numerical experiment, we consider solving the Poisson problem (36) on a 2D torus,

$$\mathbf{x} = \begin{bmatrix} (R + r \cos \theta) \cos \phi \\ (R + r \cos \theta) \sin \phi \\ r \sin \theta \end{bmatrix}, \quad 0 \leq \theta < 2\pi, \quad 0 \leq \phi < 2\pi, \quad (37)$$

where  $R$  is the distance from the center of the tube to the center of the torus and  $r < R$  is the distance from the center of the tube to the surface of the tube. In our experiment, we set  $R = 2$  and  $r = 1$ . The true solution  $u$  is set to be  $u = \sin \theta \sin \phi \frac{\partial}{\partial \theta} + \sin \theta \cos \phi \frac{\partial}{\partial \phi} \in \mathfrak{X}(M)$ . In our computation, the manufactured  $f$  is calculated by  $f := \hat{\mathbf{T}}^\top F = \hat{\mathbf{T}}^\top (a - \bar{\Delta}_B)U$ , where  $(a - \bar{\Delta}_B)U$  is an extension of  $(a - \Delta_B)u$  as defined in (26).

Numerically, the points  $\{\mathbf{x}_i\}_{i=1}^N$  are generated from the parametrization (37) using randomly sampled  $\{\theta_i, \phi_i\}_{i=1}^N$  with the uniform distribution on  $[0, 2\pi) \times [0, 2\pi)$ . We fix  $K = 51$  nearest neighbors in each local stencil. To verify the convergence over a number of points  $N = [1600, 3200, 6400, 12800, 25600]$ , we define the forward error (**FE**) and the inverse error (**IE**) in the ambient space  $\mathbb{R}^3$ , respectively, as

$$\mathbf{FE} = \max_{1 \leq i \leq N} \|\hat{\mathbf{T}}(\mathbf{x}_i)(\mathbf{L}_B \mathbf{u})_i - \mathbf{T}(\mathbf{x}_i)\Delta_B u(\mathbf{x}_i)\|_2, \quad \mathbf{IE} = \max_{1 \leq i \leq N} \|(\hat{\mathbf{T}}\hat{u})(\mathbf{x}_i) - (\mathbf{T}u)(\mathbf{x}_i)\|_2$$

where  $\|\cdot\|_2$  is the Euclidean distance, the true solution  $\mathbf{u} = (u(\mathbf{x}_1), \dots, u(\mathbf{x}_N))^\top \in \mathbb{R}^{2N \times 1}$  is a column vector,  $(\mathbf{L}_B \mathbf{u})_i \in \mathbb{R}^{2 \times 1}$  corresponds to the approximate vector value of  $\Delta_B u$  at  $\mathbf{x}_i$ ,  $\Delta_B u(\mathbf{x}_i) \in \mathbb{R}^{2 \times 1}$  is the representation in the global basis at  $\mathbf{x}_i$ ,  $\hat{u}$  is the approximate solution,  $\mathbf{T}(\mathbf{x}) = [\mathbf{t}_1(\mathbf{x}), \mathbf{t}_2(\mathbf{x})] \in \mathbb{R}^{3 \times 2}$  and  $\hat{\mathbf{T}}(\mathbf{x}) = [\hat{\mathbf{t}}_1(\mathbf{x}), \hat{\mathbf{t}}_2(\mathbf{x})] \in \mathbb{R}^{3 \times 2}$  correspond to the true and the approximate global bases, respectively. Here we push both tangent vectors on (approximate) manifolds forward to tangent vectors in  $\mathbb{R}^3$  to well-define the **FE** and **IE** in the Euclidean norm. Notice that if the manifold is known with given global bases  $\mathbf{T}(\mathbf{x})$ , then  $\mathbf{T}(\mathbf{x})$  can be ignored in the definition of **FE** and **IE** since  $\mathbf{T}: T_{i-1}\mathbf{x}O \rightarrow T_{\mathbf{x}}M$  is an isometric mapping where  $\iota$  is the local parametrization as defined in Section 4.1.

In Fig. 3, we plot the averages of **FEs** and **IEs** over 6 independent trials as functions of  $N$ . One can see that the **FEs** using degree  $l = 2, 3, 4, 5$  decrease on the order of  $N^{-(l-1)/2}$  for both the extrinsic and intrinsic methods. This numerical error rate is consistent with the GMLS error bound in (7) since the Bochner Laplacian is involved with the second-order derivative of component functions. One can further observe that the **IEs** for  $l = 3$  and  $l = 5$  decay with respective rates  $N^{-1}$  and  $N^{-2}$  as the GMLS theory predicts. Moreover, the **IEs** possess the super-convergence for degree  $l = 2$  and  $l = 4$ , that is, the **IEs** decay on the order of  $N^{-1}$  and  $N^{-2}$ , respectively, which are half-order faster than the corresponding **FEs**. This super-convergence phenomenon has also been observed in the scalar case for the Laplace-Beltrami operator of functions [33, 26].

### 5.3 Linear time-dependent equations

In this subsection, we will show the results of solving the following linear time-dependent vector-valued PDE (vector diffusion equation):

$$u_t = \nu \Delta_B u + f, \quad (\mathbf{x}, t) \in M \times (0, T] \text{ with } u(\cdot, 0) = u_0(\cdot), \quad (38)$$

where the viscosity  $\nu = 0.1$ . Here, we consider two examples of surfaces that are both isomorphic to a sphere in  $\mathbb{R}^3$ . The first example is a red blood cell (RBC) with the parametrization:

$$\mathbf{x} = \left( r \cos \theta \cos \phi, r \cos \theta \sin \phi, \frac{1}{2} \sin \theta (c_0 + c_2 \cos^2 \theta + c_4 \cos^4 \theta) \right), \quad (39)$$

where  $-\pi/2 \leq \theta \leq \pi/2$ ,  $-\pi \leq \phi < \pi$ ,  $r = 3.91/3.39$ ,  $c_0 = 0.81/3.39$ ,  $c_2 = 7.83/3.39$  and  $c_4 = -4.39/3.39$ , which is the same as the RBC in [17]. The second one is a perturbed sphere (PSP) with the parametrization:

$$\mathbf{x} = (r(\theta, \phi) \sin \theta \cos \phi, r(\theta, \phi) \sin \theta \sin \phi, r(\theta, \phi) \cos \theta), \quad (40)$$

where  $0 \leq \theta \leq \pi$ ,  $0 \leq \phi < 2\pi$  and  $r(\theta, \phi) = 1 + 0.05(1 - \cos 4\theta) \sin 2\phi$ .



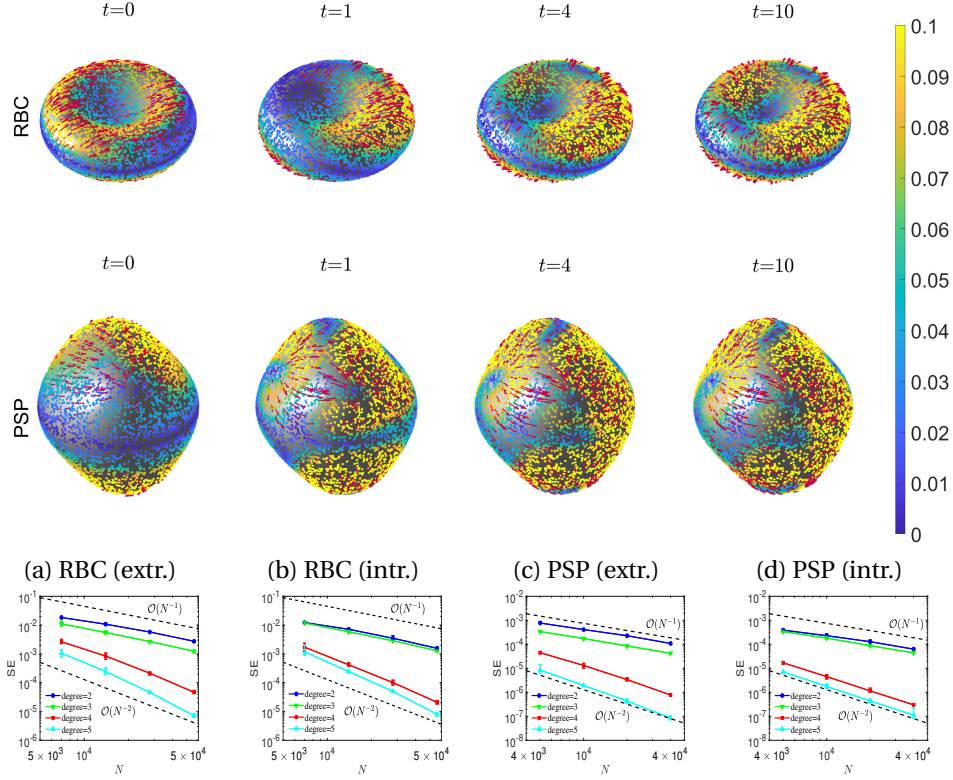


Figure 4: **Linear vector diffusion equation on RBC and PSP.** Time step  $\Delta t = 0.001$  and  $K$ -nearest neighbor  $K = 61$ . Shown in the first two rows are the randomly sampled scatter data points on RBC (the first row) and PSP (the second row) with the color bar representing the magnitude of the vector fields  $\hat{u}$  and the red arrows indicating the direction of the vector fields  $\hat{u}$ . In the third row, we show the convergence examination of the average SEs at  $t = 0.05$  with error bars obtained from the standard deviations over 6 independent trials.

In our numerical experiments, we set the external forcing  $f(\mathbf{x}, t) := \hat{\mathbf{T}}^\top \mathbf{x}$  in both examples to be time-independent. The initial condition is  $u_0(\mathbf{x}) := 0.2\hat{\mathbf{T}}^\top \mathbf{x}$  for RBC and  $u_0(\mathbf{x}) := 0.16\hat{\mathbf{T}}^\top \mathbf{x}$  for PSP. Here, the coefficients in  $u_0$  are specified such that the vector-field solutions on a scale of 0.1. To solve the time evolution equation (38), we use the GMLS method for the space discretization and the second-order explicit Runge-Kutta method for the time discretization. For both examples, we set  $K = 61$  in  $K$  nearest neighbors and the time step  $\Delta t = 0.001$ . The data are randomly sampled from the intrinsic coordinate and then mapped onto the surface using the above parametrization. To examine the convergence, we define the time-dependent solution error (SE) between true solution  $u$  and approximate solution  $\hat{u}$ :

$$\mathbf{SE} = \max_{1 \leq i \leq N} \|\hat{\mathbf{T}}(\mathbf{x}_i) \hat{u}(\mathbf{x}_i, t) - \mathbf{T}(\mathbf{x}_i) u(\mathbf{x}_i, t)\|_2.$$

In Fig. 4, we show our numerical results on RBC and PSP. In the first two rows, we show the time evolution of the extrinsic GMLS solutions on surfaces using  $N = 20000$  data points at time  $t = [0, 1, 4, 10]$ . After a sufficiently long time  $t = 10$ , we observe that the solution has arrived at its steady state given by the solution of the corresponding Poisson equation. In the last row, we show the average SEs for the numerical solutions as functions of  $N$  at time  $t = 0.05$ . To compute the reference solution, we apply the same discretization schemes over  $N = 80000$  randomly sampled points, with polynomial degree  $l = 5$ , and analytic true tangent space spanned by  $\mathbf{t}_1, \mathbf{t}_2$ . To verify the convergence, we compute the numerical solutions based on 6 independent subsampling from the 80000 randomly sampled data points with  $N = [7000, 14000, 28000, 56000]$  on RBC and  $N = [5000, 10000, 20000, 40000]$  on PSP. From the last row of Fig. 4, we can still see the super-convergence phenomena for both extrinsic formulation and intrinsic formulation in the two examples. We have also examined such super-convergence phenomena using a second-order backward differentiation formula (BDF2) [9] for time-discretization.

In addition, we also applied our GMLS approach to bumpy sphere examples which have the same parametrization form as in (40) but with the radial function  $r(\theta, \phi) = 1 + 0.05(1 - \cos w_\theta \theta) \sin w_\phi \phi$  having perturbations from higher

wavenumbers  $w_\theta, w_\phi$ . However, we found that the convergence rate becomes slower than that predicted by the GMLS theory when  $w_\theta = 6, w_\phi = 6$  and the Laplacian matrix even suffers from the eigenvalue instability when  $w_\theta, w_\phi$  become even larger [not shown here]. Notice that larger wavenumbers  $w_\theta$  and  $w_\phi$  give us a bumpy sphere with larger local curvatures. From the above numerical results, we believe that the current GMLS approach with the specified weight function in (3) can stabilize the vector Laplacians when manifolds are smooth with small curvatures. Nevertheless, when curvatures become large, the current GMLS approach may not provide a stable approximation to vector Laplacians.

#### 5.4 Viscous Burgers' equation

In this subsection, we will show the results of solving the Burgers' equation on a torus,

$$u_t + \nabla_u u = \nu \Delta_B u + f, \quad (\mathbf{x}, t) \in M \times (0, T] \text{ with } u(\cdot, 0) = u_0(\cdot), \quad (41)$$

where  $u(\cdot, t) \in \mathfrak{X}(M)$  represents a velocity field and  $\nu = 0.01$  is a viscosity parameter. In this example, the parametrization of the torus is given in (37) and the points are sampled in the same way as those in subsection 5.2. For the time discretization, we use the second-order Runge-Kutta method with  $\Delta t = 0.001$ .

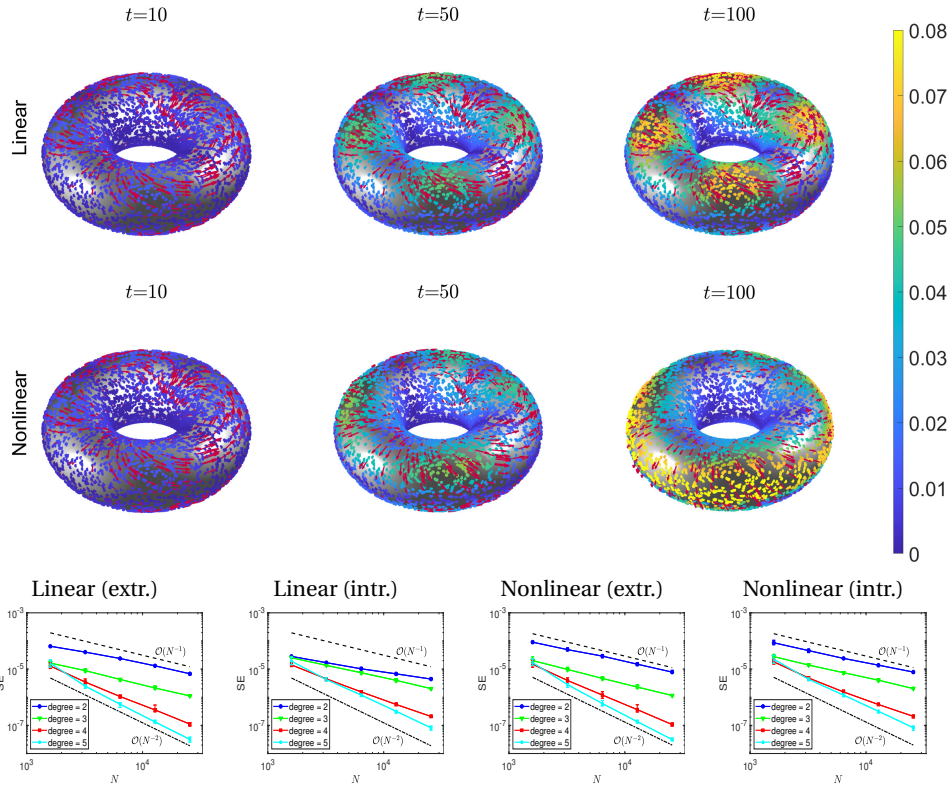


Figure 5: (Color online) **Linear vector diffusion equation and nonlinear Burgers' equation on 2D torus.** Time step  $\Delta t = 0.001$  and  $K$ -nearest neighbor  $K = 71$ . In the first two rows, we show the time evolution of the extrinsic GMLS solutions of linear (the first row) and nonlinear (the second row) equations using  $N = 6400$  randomly sampled data points on the torus, with the color bar representing the magnitude of the vector fields  $\hat{u}$  and the red arrows indicating the direction of the vector fields  $\hat{u}$ . Shown in the third row is the convergence examination of the average SEs with error bars obtained from the standard deviations over 6 independent trials at  $t = 0.05$ .

In the first two rows of Fig. 5, we show the comparison of evolution of the extrinsic GMLS solutions between the linear equation (without covariant derivative in (41)) and the nonlinear viscous Burgers' equation (with covariant derivative). For both equations, we set the same initial condition  $u_0 = 0$  to be a zero vector field and use the same external forcing  $f := -\nu \Delta_B w$  with  $w = 0.05 \sin \theta \sin \phi \frac{\partial}{\partial \theta} + 0.05 \sin \theta \cos \phi \frac{\partial}{\partial \phi}$ . In our numerical implementation for the unknown manifold, we project the forcing onto the approximate tangent bundle by multiplying by  $\hat{\mathbf{T}}^\top$  as the same in subsection 5.2. One can see from the first two rows of Fig. 5 that the solutions behave similarly for a short time ( $t = 50$ ) while they behave differently at their steady states for sufficiently long time ( $t = 100$ ). In the third row of

Fig. 5, we verify the convergence of the proposed methods for solving the linear equation and the nonlinear Burgers' equation. The true solution is set to be  $u = 0.05 \cos t \sin \theta \sin \phi \frac{\partial}{\partial \theta} + 0.05 \cos t \sin \theta \cos \phi \frac{\partial}{\partial \phi}$  for both equations. One can see that the average SEs at time  $t = 0.05$  over 6 independent trials decrease nearly on the order of  $N^{-(l-1)/2}$  for degree  $l = 2, 3, 4, 5$  as the GMLS theory predicts in (7). Here, we notice that the super-convergence phenomenon, observed previously in Section 5.3 (where the viscosity parameter  $\nu = 0.1$  was set to be relatively large), is not obviously observed here for relatively small viscosity  $\nu = 0.01$  in both the linear and nonlinear regimes.

In addition, we numerically simulated the regime for the external forcing with large amplitude. We observed that shock waves are first formed in the solution and then the solution suffers from numerical instability [not shown here]. We also numerically observed such instability results by using the Crank-Nicolson/Adams-Bashforth scheme [29]. The reason is that in the local hypothesis space only containing multi-variate polynomials, it cannot capture the discontinuous solution such as shock waves well.

## 6 Conclusions and discussion

In this paper, we extended the GMLS approach using both intrinsic formulation and extrinsic formulation for approximating vector Laplacians and covariant derivative and further for solving vector-valued PDEs on unknown smooth 2D manifolds, identified by a randomly-sampled data point cloud. The scheme can reach an arbitrary-order algebraic accuracy on smooth manifolds with small curvatures. For the intrinsic method, we approximated the geometry quantities, functions, and their derivatives in the local Monge coordinate system to simplify the intrinsic formulation of the Bochner Laplacian in (18). Then we transformed the representation of GMLS weights from the local tangent-vector basis to the global tangent-vector basis in order to assemble these weights into the sparse  $2N \times 2N$  Bochner Laplacian matrix. For the extrinsic method, we saved the memory cost and computational cost in approximating the Bochner Laplacian and covariant derivative, which improved our previous results in [22]. In particular, we applied the GMLS approach to make the discretization sparse and we also reduced the dimension of Laplacian matrices as well as the nonzero entries in the matrices by applying an appropriate projection.

There are several remaining questions for future investigation. First, the stability problem still exists in the GMLS method for approximating the vector Laplacians on manifolds with high curvatures (such as bumpy spheres discussed in Section 5.3). Second, the GMLS approach whose hypothesis space only contains multivariate polynomials may fail to approximate discontinuous solutions such as shock waves of nonlinear Burgers' equation. Third, it is of interest to solve vector-valued PDEs with classical boundary conditions on manifolds with boundaries identified with randomly sampled data points.

## Acknowledgments

S. J. was supported by the NSFC Grant No. 12101408. Q. Y. was supported by the Simons Foundation grant 601937, DNA. We would like to thank John Harlim for helpful comments.

## A Intrinsic formulation for other vector Laplacians

In this section, we first review some concepts and notations from intrinsic differential geometry [30, 55]. Then we discuss the intrinsic GMLS approximation of the L Laplacian (which involves the symmetric stress tensor) and Hodge Laplacian (which involves the anti-symmetric stress tensor) acting on vector fields.

### A.1 Intrinsic Differential Geometry

Let  $M$  be a  $d$ -dimensional Riemannian manifold with a local coordinate  $(\xi^1, \dots, \xi^d)$  defined on an open subset  $O$  in  $M$ . The Riemannian metric is  $g = g_{ij} d\xi^i \otimes d\xi^j$  with the components  $g_{ij} = \langle \partial_i, \partial_j \rangle$ , where  $\partial_i = \frac{\partial}{\partial \xi^i}$  is the  $i$ th coordinate vector field and  $(d\xi^1, \dots, d\xi^d)$  is the associated coordinate coframe. Recall that  $d\xi^j(\partial_i) = \delta_i^j$ , where  $\delta_i^j$  is the delta function.

To define the vector Laplacian, we first introduce the concepts for the gradient operator and the divergence operator. Let  $u = \tilde{u}^i \partial_i \in \mathfrak{X}(M)$  be a vector field and let  $\nabla$  be the Levi-Civita connection. Then the covariant differentiation is defined as

$$\nabla u = \tilde{u}_{;j}^i \frac{\partial}{\partial \xi^i} \otimes d\xi^j$$

where  $\tilde{u}^i_{;j} = \frac{\partial \tilde{u}^i}{\partial \xi^j} + \tilde{u}^k \Gamma^i_{jk}$ , and the gradient of the vector field is defined to be a (2, 0) tensor field as in (24),

$$\text{grad}_g u = \sharp \nabla u = g^{kj} \tilde{u}^i_{;k} \frac{\partial}{\partial \xi^i} \otimes \frac{\partial}{\partial \xi^j}.$$

For a vector field  $u$ , its divergence can be expressed as

$$\text{div}_g(u) = \text{tr}(\nabla u) = \tilde{u}^i_{;i}.$$

Let  $v = \tilde{v}^{ij} \partial_i \otimes \partial_j \in \mathfrak{X}(M) \times \mathfrak{X}(M)$  be a (2, 0) tensor field. One can define the divergence of a (2, 0) tensor field (see e.g. Ch 2 in [55]):

$$\text{div}_g(v) := \text{tr}_1^2(\nabla v) = \text{tr}_1^2\left(\tilde{v}^{ij} \frac{\partial}{\partial \xi^i} \otimes \frac{\partial}{\partial \xi^j} \otimes d\xi^k\right) = \tilde{v}^{ik} \partial_i, \quad (42)$$

where the trace operator  $\text{tr}_1^2$  is taken on the *last two indices* of the tensor field  $\nabla v$ .

We now present the intrinsic formulation for the three Laplacians acting on vector fields: 1) the Bochner Laplacian, 2) the L Laplacian which involves the symmetric surface stress tensor, and 3) the Hodge Laplacian. We concern these three Laplacians here since they are the candidates for the diffusion operators in Navier-Stokes equations on Riemannian manifolds as discussed in references [7, 46, 56].

1) The Bochner Laplacian acting on a vector field  $u = \tilde{u}^k \partial_k$  is defined as

$$\Delta_B u := \text{div}_g(\text{grad}_g u) = \text{div}_g\left(g^{kj} \tilde{u}^i_{;k} \frac{\partial}{\partial \xi^i} \otimes \frac{\partial}{\partial \xi^j}\right) = g^{kj} \tilde{u}^i_{;kj} \partial_i. \quad (43)$$

2) For the L laplacian, one can first define the symmetric deformation rate tensor  $S$  (cf. [7, 46] or Ch 17 in [56]),

$$S := \frac{1}{2} \left( \text{grad}_g u + (\text{grad}_g u)^\top \right) = \frac{1}{2} \left( g^{mj} \tilde{u}^i_{;m} + g^{mi} \tilde{u}^j_{;m} \right) \partial_i \otimes \partial_j.$$

Then the (negative-definite) L Laplacian acting on the vector field  $u$  can be defined and computed in the local coordinates as

$$\Delta_L u := 2\text{div}_g(S) = \text{div}_g\left(\text{grad}_g u + (\text{grad}_g u)^\top\right) = \left(g^{ij} \tilde{u}^k_{;ij} + g^{ki} \tilde{u}^j_{;ij}\right) \partial_k. \quad (44)$$

3) The (negative-definite) Hodge Laplacian acting on the vector field  $u = \tilde{u}^k \partial_k$  is defined as

$$\Delta_H u := -\sharp(d^* d + dd^*)\flat u,$$

where  $d$  is the exterior derivative,  $d^*$  is the formal adjoint of  $d$ , and the symbols  $\sharp$  and  $\flat$  are the standard musical isomorphisms. By this definition, the Hodge Laplacian can be expressed and computed as

$$\begin{aligned} \Delta_H u &= \text{div}_g(\text{grad}_g u - (\text{grad}_g u)^\top) + \text{grad}_g(\text{div}_g(u)) \\ &= \left(g^{ij} \tilde{u}^k_{;ij} - g^{kj} \tilde{u}^i_{;ji} + g^{jk} \tilde{u}^i_{;ij}\right) \partial_k. \end{aligned} \quad (45)$$

## A.2 Intrinsic GMLS approximation of other vector Laplacians

In this section, we first provide the representation of  $\Delta_L u$  and  $\Delta_H u$  in the Monge coordinate system following the similar computational procedure for the Bochner  $\Delta_B u$  in Section 3.2.1. Recall that the notations,  $\{a_{\alpha_1, \alpha_2} | 2 \leq \alpha_1 + \alpha_2 \leq l\}$ , are the regression coefficients of the parameterized surface (see equation (9)), and the notations,  $\beta_{\alpha_1, \alpha_2}$  and  $\gamma_{\alpha_1, \alpha_2}$  for  $0 \leq \alpha_1 + \alpha_2 \leq l$ , are the coefficients of respective component,  $\tilde{u}^1$  and  $\tilde{u}^2$ , of the vector field  $u = \tilde{u}^k \partial_k$  (see equation (17)).

Then the L Laplacian in (44) at the base point  $\mathbf{x}_0$  can be approximated as

$$\begin{aligned} &\Delta_L u(\mathbf{x}_0) \\ &= (g^{ij} \tilde{u}^k_{;ij} + g^{ki} \tilde{u}^j_{;ij}) \partial_k |_{\mathbf{x}_0} = \left[ (2\tilde{u}^1_{;11} + \tilde{u}^1_{;22} + \tilde{u}^2_{;12}) \partial_1 + (\tilde{u}^2_{;11} + \tilde{u}^1_{;21} + 2\tilde{u}^2_{;22}) \partial_2 \right] |_{\mathbf{x}_0} \\ &= \left( 4\beta_{2,0} + 2\beta_{0,2} + \beta_{0,0} \left[ 8(a_{2,0})^2 + (a_{1,1})^2 + 4a_{0,2}a_{2,0} \right] + \gamma_{1,1} + \gamma_{0,0} \left[ 4a_{2,0}a_{1,1} + 4a_{0,2}a_{1,1} \right] \right) \partial_1 |_{\mathbf{x}_0} \\ &\quad + \left( \beta_{1,1} + \beta_{0,0} \left[ 4a_{2,0}a_{1,1} + 4a_{0,2}a_{1,1} \right] + 4\gamma_{0,2} + 2\gamma_{2,0} + \gamma_{0,0} \left[ 8(a_{0,2})^2 + (a_{1,1})^2 + 4a_{2,0}a_{2,0} \right] \right) \partial_2 |_{\mathbf{x}_0}. \end{aligned}$$

The Hodge Laplacian in (45) can be approximated as

$$\begin{aligned}
\Delta_H u(\mathbf{x}_0) &= (g^{ij} \bar{u}_{;ij}^k - g^{kj} \bar{u}_{;ji}^i + g^{jk} \bar{u}_{;ij}^i) \partial_k |_{\mathbf{x}_0} \\
&= \left[ (\bar{u}_{;22}^1 - \bar{u}_{;12}^2 + \bar{u}_{;11}^1 + \bar{u}_{;21}^2) \partial_1 + (\bar{u}_{;11}^2 - \bar{u}_{;21}^1 + \bar{u}_{;12}^1 + \bar{u}_{;22}^2) \partial_2 \right] |_{\mathbf{x}_0} \\
&= \left( 2\beta_{2,0} + 2\beta_{0,2} + \beta_{0,0} \left[ 4(a_{2,0})^2 + 2(a_{1,1})^2 - 4a_{0,2}a_{2,0} \right] + \gamma_{0,0} \left[ 2a_{2,0}a_{1,1} + 2a_{0,2}a_{1,1} \right] \right) \partial_1 |_{\mathbf{x}_0} \\
&\quad + \left( \beta_{0,0} \left[ 2a_{2,0}a_{1,1} + 2a_{0,2}a_{1,1} \right] + 2\gamma_{0,2} + 2\gamma_{2,0} + \gamma_{0,0} \left[ 4(a_{0,2})^2 + 2(a_{1,1})^2 - 4a_{2,0}a_{2,0} \right] \right) \partial_2 |_{\mathbf{x}_0}.
\end{aligned}$$

Then one can follow the similar GMLS procedure in Section 3.2 to approximate  $\Delta_L u$  and  $\Delta_H u$  on a point cloud.

## B Extrinsic formulation for other vector Laplacians

In this section, we first supplement some details for the extrinsic formulation of the Bochner Laplacian as in [22]. Then, we review the extrinsic formulation result for the L Laplacian and the Hodge Laplacian acting on vector fields [22] and provide the extrinsic GMLS approximation of the two vector Laplacians. In the following, we use the notations introduced in Section 4.1 and Section 4.2.

### B.1 Bochner Laplacian

Here, we supplement a detailed derivation of the extrinsic formulation for the Bochner Laplacian in Section 4.1. Let  $v = v^{jk} \frac{\partial}{\partial \xi^j} \otimes \frac{\partial}{\partial \xi^k} \in \mathfrak{X}(M) \times \mathfrak{X}(M)$  be a (2,0) tensor field, and let

$$V = \frac{\partial X^s}{\partial \xi^j} v^{jk} \frac{\partial X^t}{\partial \xi^k} \frac{\partial}{\partial X^s} \otimes \frac{\partial}{\partial X^t} := V^{st} \frac{\partial}{\partial X^s} \otimes \frac{\partial}{\partial X^t},$$

be a smooth extension of  $v$  onto an open subset in  $\mathbb{R}^3$  such that  $V|_M = v$ . In general, the tensor field  $v$  is not symmetric, that is,  $v^{jk} \neq v^{kj}$ . We now consider the extrinsic formulation for the divergence of a (2,0) tensor field  $v$ . Using the definition in (42), one can verify the identity extension formulation for the divergence (see e.g. [22]),

$$\operatorname{div}_g(v) = \mathbf{P} \operatorname{tr}_1^2(\mathbf{P} \bar{\nabla}_{\mathbb{R}^3}(V)) = \mathbf{P} \operatorname{tr}_1^2(\mathcal{G}_r V^{st} \frac{\partial}{\partial X^s} \otimes \frac{\partial}{\partial X^t} \otimes dX^r) = \mathbf{P} \left( \mathcal{G}_t V^{st} \frac{\partial}{\partial X^s} \right),$$

where  $\mathcal{G}_r = (\mathbf{e}_r \cdot \mathbf{P}) \cdot \bar{\nabla}_{\mathbb{R}^3} = (\mathbf{e}_r \cdot \mathbf{P}) \cdot \overline{\operatorname{grad}}_{\mathbb{R}^3}$  is the differential operator defined in (22). In matrix form, above equation can be written as

$$\begin{aligned}
\operatorname{div}_g(v) &= \mathbf{P} \begin{bmatrix} \sum_{k=1}^3 \mathcal{G}_k V^{1k} \\ \sum_{k=1}^3 \mathcal{G}_k V^{2k} \\ \sum_{k=1}^3 \mathcal{G}_k V^{3k} \end{bmatrix} = \mathbf{P} \begin{bmatrix} \mathcal{G}_1 & & \\ & \mathcal{G}_1 & \\ & & \mathcal{G}_1 \end{bmatrix} \begin{bmatrix} V^{11} \\ V^{21} \\ V^{31} \end{bmatrix} + \dots + \mathbf{P} \begin{bmatrix} \mathcal{G}_3 & & \\ & \mathcal{G}_3 & \\ & & \mathcal{G}_3 \end{bmatrix} \begin{bmatrix} V^{13} \\ V^{23} \\ V^{33} \end{bmatrix} \\
&= \mathcal{H}_1 \begin{bmatrix} V^{11} \\ V^{21} \\ V^{31} \end{bmatrix} + \mathcal{H}_2 \begin{bmatrix} V^{12} \\ V^{22} \\ V^{32} \end{bmatrix} + \mathcal{H}_3 \begin{bmatrix} V^{13} \\ V^{23} \\ V^{33} \end{bmatrix} := \mathcal{H}_1 V|_1 + \mathcal{H}_2 V|_2 + \mathcal{H}_3 V|_3
\end{aligned} \tag{46}$$

where  $\mathcal{H}_s$  is defined as in (25) and  $V|_s := (V^{1s}, V^{2s}, V^{3s})^\top$  is the sth column of tensor field  $V$  for  $s = 1, 2, 3$ .

Let  $v = \operatorname{grad}_g u \in \mathfrak{X}(M) \times \mathfrak{X}(M)$  be the gradient of a vector field which is a (2,0) tensor field. Using the extrinsic formulation in (24), one obtains the equation:

$$V = (V|_1, V|_2, V|_3) = (\mathcal{H}_1 U, \mathcal{H}_2 U, \mathcal{H}_3 U) = \mathbf{P} \left( \overline{\operatorname{grad}}_{\mathbb{R}^3} U \right) \mathbf{P},$$

which gives us

$$V|_k = \mathcal{H}_k U, \quad \text{for } k = 1, 2, 3. \tag{47}$$

Combining (46) and (47), one can obtain the extrinsic formulation for the Bochner Laplacian of a vector field,  $\Delta_B u = g^{ij} u_{;ij}^k \frac{\partial}{\partial \xi^k} = \operatorname{div}_g(\operatorname{grad}_g u)$ , as

$$\begin{aligned}
\Delta_B u &= \operatorname{div}_g(\operatorname{grad}_g u) = \operatorname{div}_g(v) = \mathcal{H}_1 V|_1 + \mathcal{H}_2 V|_2 + \mathcal{H}_3 V|_3 \\
&= \mathcal{H}_1 \mathcal{H}_1 U + \mathcal{H}_2 \mathcal{H}_2 U + \mathcal{H}_3 \mathcal{H}_3 U := \bar{\Delta}_B U.
\end{aligned}$$

## B.2 L Laplacian

We first review the extrinsic formulation for the L Laplacian (see e.g. [52, 22]). Let  $v = \text{grad}_g u$  be the gradient of a vector field  $u$  and let  $V$  be a smooth extension of  $v$  onto an open subset in  $\mathbb{R}^3$  such that  $V|_M = v$ . Based on the definition of the L Laplacian in (44), one can obtain the extrinsic formulation for the L Laplacian:

$$\begin{aligned} \Delta_L u &= \text{div}_g(v + v^\top) = \text{Ptr}_1^2(\mathbf{P}\tilde{\mathbf{V}}_{\mathbb{R}^3}(V + V^\top)) = \mathbf{P} \begin{bmatrix} \sum_{k=1}^3 \mathcal{G}_k (V^{1k} + V^{k1}) \\ \sum_{k=1}^3 \mathcal{G}_k (V^{2k} + V^{k2}) \\ \sum_{k=1}^3 \mathcal{G}_k (V^{3k} + V^{k3}) \end{bmatrix} \\ &= \mathcal{H}_1 [V|_1 + (\tilde{V}_1)^\top] + \mathcal{H}_2 [V|_2 + (\tilde{V}_2)^\top] + \mathcal{H}_3 [V|_3 + (\tilde{V}_3)^\top], \end{aligned} \quad (48)$$

where  $\tilde{V}_i = [V_{i1}, V_{i2}, V_{i3}]$  is the  $i$ th row of the  $(2,0)$  tensor field  $V$  for  $i = 1, 2, 3$ . Here, we have used the notations  $\mathcal{G}_j$  in (22) and  $\mathcal{H}_j$  in (25) for  $j = 1, 2, 3$ , and we can further calculate  $\tilde{V}^i$  as

$$\begin{aligned} (\tilde{V}^i)^\top &= [V_{i1}, V_{i2}, V_{i3}]^\top = \begin{bmatrix} P_{i1} & P_{i2} & P_{i3} \\ \mathcal{G}_1 U^1 & \mathcal{G}_2 U^1 & \mathcal{G}_3 U^1 \\ \mathcal{G}_1 U^2 & \mathcal{G}_2 U^2 & \mathcal{G}_3 U^2 \\ \mathcal{G}_1 U^3 & \mathcal{G}_2 U^3 & \mathcal{G}_3 U^3 \end{bmatrix}^\top \\ &= \begin{bmatrix} P_{i1} \mathcal{G}_1 & P_{i2} \mathcal{G}_1 & P_{i3} \mathcal{G}_1 \\ P_{i1} \mathcal{G}_2 & P_{i2} \mathcal{G}_2 & P_{i3} \mathcal{G}_2 \\ P_{i1} \mathcal{G}_3 & P_{i2} \mathcal{G}_3 & P_{i3} \mathcal{G}_3 \end{bmatrix} \begin{bmatrix} U^1 \\ U^2 \\ U^3 \end{bmatrix} := \mathcal{S}_i U. \end{aligned} \quad (49)$$

Substituting (49) into (48), we obtain

$$\Delta_L u = \mathcal{H}_1 [\mathcal{H}_1 + \mathcal{S}_1] U + \dots + \mathcal{H}_3 [\mathcal{H}_3 + \mathcal{S}_3] U := \tilde{\Delta}_L U.$$

For the discretization, one can approximate the differential operator  $\mathcal{S}_i$  in the stencil as,

$$\mathbf{S}_i = \begin{bmatrix} \text{diag}(\mathbf{p}_{i1}) \mathbf{G}_1 & \text{diag}(\mathbf{p}_{i2}) \mathbf{G}_1 & \text{diag}(\mathbf{p}_{i3}) \mathbf{G}_1 \\ \text{diag}(\mathbf{p}_{i1}) \mathbf{G}_2 & \text{diag}(\mathbf{p}_{i2}) \mathbf{G}_2 & \text{diag}(\mathbf{p}_{i3}) \mathbf{G}_2 \\ \text{diag}(\mathbf{p}_{i1}) \mathbf{G}_3 & \text{diag}(\mathbf{p}_{i2}) \mathbf{G}_3 & \text{diag}(\mathbf{p}_{i3}) \mathbf{G}_3 \end{bmatrix}_{3K \times 3K}, \quad (50)$$

where  $\mathbf{p}_{ij} = (P_{ij}(\mathbf{x}_{0,1}), \dots, P_{ij}(\mathbf{x}_{0,K})) \in \mathbb{R}^{K \times 1}$  for  $1 \leq i, j \leq 3$ . Then, the L Laplacian can be subsequently approximated in the stencil  $S_{\mathbf{x}_0}$  as,

$$\Delta_L u|_{S_{\mathbf{x}_0}} = \tilde{\Delta}_L U|_{S_{\mathbf{x}_0}} = \sum_{\ell=1}^3 \mathcal{H}_\ell (\mathcal{H}_\ell + \mathcal{S}_\ell) U|_{S_{\mathbf{x}_0}} \approx \sum_{\ell=1}^3 \mathbf{H}_\ell (\mathbf{H}_\ell + \mathbf{S}_\ell) \mathbf{U}_{\mathbf{x}_0}, \quad (51)$$

where  $\mathbf{U}_{\mathbf{x}_0}$  has been defined in (30).

We now consider the reduction for the L Laplacian following the similar procedure to the Bochner Laplacian as in Section 4.3. Using the definition of  $\mathbf{H}_i$  in (29) and  $\mathbf{S}_i$  in (50), one can write the L Laplacian in the stencil  $S_{\mathbf{x}_0}$  as

$$\Delta_L u|_{S_{\mathbf{x}_0}} \approx \sum_{\ell=1}^3 \mathbf{H}_\ell (\mathbf{H}_\ell + \mathbf{S}_\ell) \mathbf{U}_{\mathbf{x}_0} = \sum_{\ell=1}^3 \mathbf{P}^\otimes \mathbf{H}_\ell \mathbf{P}^\otimes (\mathbf{H}_\ell + \mathbf{S}_\ell) \mathbf{P}^\otimes \mathbf{U}_{\mathbf{x}_0},$$

where made use of  $\mathbf{P}^\otimes \mathbf{S}_\ell = \mathbf{S}_\ell$  since each column of  $\mathbf{S}_\ell$  always lives in the tangent bundle of  $M$ . Using the decomposition  $\mathbf{P}^\otimes = \mathbf{T}^\otimes \mathbf{T}^{\otimes \top}$ , one arrives at

$$\begin{aligned} \Delta_L u|_{S_{\mathbf{x}_0}} &\approx \sum_{\ell=1}^3 \mathbf{T}^\otimes (\mathbf{T}^{\otimes \top} \mathbf{H}_\ell \mathbf{T}^\otimes) [\mathbf{T}^{\otimes \top} (\mathbf{H}_\ell + \mathbf{S}_\ell) \mathbf{T}^\otimes] (\mathbf{T}^{\otimes \top} \mathbf{U}_{\mathbf{x}_0}) \\ &:= \mathbf{T}^\otimes \left[ \sum_{\ell=1}^3 \mathbf{R}_\ell (\mathbf{R}_\ell + \mathbf{M}_\ell) \right] (\mathbf{T}^{\otimes \top} \mathbf{U}_{\mathbf{x}_0}), \end{aligned} \quad (52)$$

where  $\mathbf{R}_\ell := \mathbf{T}^{\otimes \top} \mathbf{H}_\ell \mathbf{T}^\otimes = \mathbf{T}^{\otimes \top} (\mathbf{I}_3 \otimes \mathbf{G}_\ell) \mathbf{T}^\otimes$  has been defined in (32),  $\mathbf{M}_\ell := \mathbf{T}^{\otimes \top} \mathbf{S}_\ell \mathbf{T}^\otimes$  is the reduction of  $\mathbf{S}_\ell$ , and  $\sum_{\ell=1}^3 \mathbf{R}_\ell (\mathbf{R}_\ell + \mathbf{M}_\ell) \in \mathbb{R}^{2K \times 2K}$  is the L Laplacian matrix that maps the coordinate representation of  $u|_{S_{\mathbf{x}_0}}$  to the coordinate representation of  $(\Delta_L u)|_{S_{\mathbf{x}_0}}$  w.r.t. the global basis  $\{\mathbf{t}_j(\mathbf{x}_{0,k})\}_{j=1,2}^{k=1,\dots,K}$ .

Next, we compute the differential matrix  $\mathbf{M}_\ell$  componentwisely. Fix some  $\ell$ , one can compute a  $2 \times 2$  block matrix component of  $\mathbf{M}_\ell$  whose rows corresponding to  $\mathbf{x}_{0,s}$  and columns corresponding to  $\mathbf{x}_{0,t}$ ,

$$\begin{aligned} &\begin{bmatrix} \mathbf{t}_1(\mathbf{x}_{0,s})^\top \\ \mathbf{t}_2(\mathbf{x}_{0,s})^\top \end{bmatrix}_{2 \times 3} \begin{bmatrix} P_{\ell 1}(\mathbf{x}_{0,s}) (\mathbf{G}_1)_{st} & P_{\ell 2}(\mathbf{x}_{0,s}) (\mathbf{G}_1)_{st} & P_{\ell 3}(\mathbf{x}_{0,s}) (\mathbf{G}_1)_{st} \\ P_{\ell 1}(\mathbf{x}_{0,s}) (\mathbf{G}_2)_{st} & P_{\ell 2}(\mathbf{x}_{0,s}) (\mathbf{G}_2)_{st} & P_{\ell 3}(\mathbf{x}_{0,s}) (\mathbf{G}_2)_{st} \\ P_{\ell 1}(\mathbf{x}_{0,s}) (\mathbf{G}_3)_{st} & P_{\ell 2}(\mathbf{x}_{0,s}) (\mathbf{G}_3)_{st} & P_{\ell 3}(\mathbf{x}_{0,s}) (\mathbf{G}_3)_{st} \end{bmatrix} \begin{bmatrix} \mathbf{t}_1(\mathbf{x}_{0,t}) & \mathbf{t}_2(\mathbf{x}_{0,t}) \end{bmatrix}_{3 \times 2} \\ &= \left( \begin{bmatrix} \mathbf{t}_1(\mathbf{x}_{0,s})^\top \\ \mathbf{t}_2(\mathbf{x}_{0,s})^\top \end{bmatrix} \begin{bmatrix} (\mathbf{G}_1)_{st} \\ (\mathbf{G}_2)_{st} \\ (\mathbf{G}_3)_{st} \end{bmatrix} \right) \left( \begin{bmatrix} P_{\ell 1}(\mathbf{x}_{0,s}) & P_{\ell 2}(\mathbf{x}_{0,s}) & P_{\ell 3}(\mathbf{x}_{0,s}) \end{bmatrix} \begin{bmatrix} \mathbf{t}_1(\mathbf{x}_{0,t}) & \mathbf{t}_2(\mathbf{x}_{0,t}) \end{bmatrix} \right) := \hat{\mathbf{M}}_{st}^\ell. \end{aligned}$$



Stacking all these block matrices  $\{\hat{\mathbf{M}}_{st}^\ell\}_{s,t=1}^K$  for each  $\ell = 1, 2, 3$ , one can obtain a reshaping of  $\mathbf{M}_\ell$  via some appropriate row and column interchanges. Therefore, the weights  $\{\mathbf{w}^k \in \mathbb{R}^{2 \times 2}\}_{k=1}^K$  for approximating the L Laplacian at the base  $\mathbf{x}_0$  corresponding to the 2 rows of the matrix  $\sum_{\ell=1}^3 \mathbf{R}_\ell (\mathbf{R}_\ell + \mathbf{M}_\ell)$  in (52) become

$$(\mathbf{w}^1, \dots, \mathbf{w}^K) = \sum_{\ell=1}^3 (\hat{\mathbf{R}}_{11}^\ell, \dots, \hat{\mathbf{R}}_{1K}^\ell) \begin{bmatrix} \hat{\mathbf{R}}_{11}^\ell + \hat{\mathbf{M}}_{11}^\ell & \dots & \hat{\mathbf{R}}_{1K}^\ell + \hat{\mathbf{M}}_{1K}^\ell \\ \vdots & \ddots & \vdots \\ \hat{\mathbf{R}}_{K1}^\ell + \hat{\mathbf{M}}_{K1}^\ell & \dots & \hat{\mathbf{R}}_{KK}^\ell + \hat{\mathbf{M}}_{KK}^\ell \end{bmatrix} \in \mathbb{R}^{2 \times 2K}.$$

Here, these weights satisfy  $\Delta_L u(\mathbf{x}_0) \approx \sum_{k=1}^K \mathbf{w}^k u(\mathbf{x}_{0,k})$  at the base point  $\mathbf{x}_0$ .

### B.3 Hodge Laplacian

We now review the extrinsic formulation for the Hodge Laplacian [22], which can be written as

$$\Delta_H u = \mathbf{P} \text{tr}_1^2 (\mathbf{P} \bar{\mathbf{V}}_{\mathbb{R}^3} (V - V^\top)) + \overline{\mathbf{P} \text{grad}_{\mathbb{R}^3}} (\text{tr}_1^1 [\mathbf{P} \bar{\mathbf{V}}_{\mathbb{R}^3} U]), \quad (53)$$

where  $V = \mathbf{P} \left( \overline{\text{grad}_{\mathbb{R}^3}} U \right) \mathbf{P}$  is an extension of  $v = \text{grad}_g u$  such that  $V|_M = v$ . We note that the first term in above (53) is only different from the extrinsic formulation for the L Laplacian in (48) by a negative sign. Thus, it only remains to compute the last term in (53),

$$\overline{\mathbf{P} \text{grad}_{\mathbb{R}^3}} (\text{tr}_1^1 [\mathbf{P} \bar{\mathbf{V}}_{\mathbb{R}^3} U]) = \overline{\mathbf{P} \text{grad}_{\mathbb{R}^3}} \left( \sum_{k=1}^3 \mathcal{G}_k U^k \right) = \begin{bmatrix} \mathcal{G}_1 \\ \mathcal{G}_2 \\ \mathcal{G}_3 \end{bmatrix} [\mathcal{G}_1, \mathcal{G}_2, \mathcal{G}_3] \begin{bmatrix} U^1 \\ U^2 \\ U^3 \end{bmatrix}. \quad (54)$$

For the discretization, one only needs to substitute each  $\mathcal{G}_i$  above with the differential matrix  $\mathbf{G}_i$  for  $i = 1, 2, 3$ .

Next, we only need to consider the dimension reduction for the discretization of equation (54). Using the decomposition  $\mathbf{P}^\otimes = \mathbf{T}^\otimes \mathbf{T}^{\otimes \top}$ , we arrive at

$$\begin{aligned} \overline{\mathbf{P} \text{grad}_{\mathbb{R}^3}} (\text{tr}_1^1 [\mathbf{P} \bar{\mathbf{V}}_{\mathbb{R}^3} U])|_{S_{\mathbf{x}_0}} &\approx \mathbf{T}^\otimes \left( \mathbf{T}^{\otimes \top} \begin{bmatrix} \mathbf{G}_1 \\ \mathbf{G}_2 \\ \mathbf{G}_3 \end{bmatrix} \right) ([\mathbf{G}_1, \mathbf{G}_2, \mathbf{G}_3] \mathbf{T}^\otimes) (\mathbf{T}^{\otimes \top} \mathbf{U}_{\mathbf{x}_0}) \\ &:= \mathbf{T}^\otimes \mathbf{J} (\mathbf{T}^{\otimes \top} \mathbf{U}_{\mathbf{x}_0}). \end{aligned}$$

Thus, the Hodge Laplacian can be approximated as

$$\Delta_H u|_{S_{\mathbf{x}_0}} \approx \mathbf{T}^\otimes \left( \left[ \sum_{\ell=1}^3 \mathbf{R}_\ell (\mathbf{R}_\ell - \mathbf{M}_\ell) \right] + \mathbf{J} \right) (\mathbf{T}^{\otimes \top} \mathbf{U}_{\mathbf{x}_0}).$$

Let  $(\hat{\mathbf{J}}_{11}, \dots, \hat{\mathbf{J}}_{1K}) \in \mathbb{R}^{2 \times 2K}$  be the 2 rows of  $\mathbf{J}$  corresponding to the approximation of  $\Delta_H u$  at the base point  $\mathbf{x}_0$ . Then, the weights  $\{\mathbf{w}^k \in \mathbb{R}^{2 \times 2}\}_{k=1}^K$  for the Hodge Laplacian become

$$(\mathbf{w}^1, \dots, \mathbf{w}^K) = \sum_{\ell=1}^3 (\hat{\mathbf{R}}_{11}^\ell, \dots, \hat{\mathbf{R}}_{1K}^\ell) \begin{bmatrix} \hat{\mathbf{R}}_{11}^\ell - \hat{\mathbf{M}}_{11}^\ell & \dots & \hat{\mathbf{R}}_{1K}^\ell - \hat{\mathbf{M}}_{1K}^\ell \\ \vdots & \ddots & \vdots \\ \hat{\mathbf{R}}_{K1}^\ell - \hat{\mathbf{M}}_{K1}^\ell & \dots & \hat{\mathbf{R}}_{KK}^\ell - \hat{\mathbf{M}}_{KK}^\ell \end{bmatrix} + (\hat{\mathbf{J}}_{11}, \dots, \hat{\mathbf{J}}_{1K}),$$

which are the 2 rows of the matrix  $\sum_{\ell=1}^3 \mathbf{R}_\ell (\mathbf{R}_\ell - \mathbf{M}_\ell) + \mathbf{J}$  corresponding to the base point  $\mathbf{x}_0$  such that  $\Delta_H u(\mathbf{x}_0) \approx \sum_{k=1}^K \mathbf{w}^k u(\mathbf{x}_{0,k})$ .

## References

- [1] D. Álvarez, P. González-Rodríguez, and M. Kindelan. A local radial basis function method for the laplace-beltrami operator. *J. Sci. Comput.*, 86, 2021.
- [2] D. N. Arnold, R. S. Falk, and R. Winther. Finite element exterior calculus: from Hodge theory to numerical stability. *Bull. Amer. Math. Soc.*, 47(2):281–354, 2010.
- [3] O. Azencot, M. Ovsjanikov, F. Chazal, and M. Ben-Chen. Discrete derivatives of vector fields on surfaces - an operator approach. *ACM Trans. Graph.s*, 34(3):1–13, 2015.



- [4] J. W. Barrett, H. Garcke, and R. Nürnberg. Numerical computations of the dynamics of fluidic membranes and vesicles. *Phys. Rev. E*, 92(5):052704, 2015.
- [5] T. Berry and D. Giannakis. Spectral exterior calculus. *Comm. Pure Appl. Math.*, 73(4):689–770, 2020.
- [6] M. Bertalmio, L.-T. Cheng, S. Osher, and G. Sapiro. Variational problems and partial differential equations on implicit surfaces. *J. Comput. Phys.*, 174(2):759–780, 2001.
- [7] C. H. Chan, M. Czubak, and M. M. Disconzi. The formulation of the navier-stokes equations on riemannian manifolds. *J. Geom. Phys.*, 121:335–346, 2017.
- [8] K. Crane, M. Desbrun, and P. Schröder. Trivial connections on discrete surfaces. In *Computer Graphics Forum*, volume 29, pages 1525–1533. Wiley Online Library, 2010.
- [9] C. F. Curtiss and J. O. Hirschfelder. Integration of stiff equations. *Proc. Natl. Acad. Sci.*, 38(3):235–243, 1952.
- [10] M. Desbrun, E. Kanso, and Y. Tong. Discrete differential forms for computational modeling. In *ACM SIGGRAPH 2006 Courses*, pages 39–54. 2006.
- [11] M. P. Do Carmo. *Riemannian geometry*, volume 6. Springer, 1992.
- [12] D. L. Donoho and C. Grimes. Hessian eigenmaps: Locally linear embedding techniques for high-dimensional data. *Proc. Natl. Acad. Sci.*, 100(10):5591–5596, 2003.
- [13] N. Flyer and B. Fornberg. Solving pdes with radial basis functions. *Acta Numerica*, 24:215–258, 2015.
- [14] N. Flyer, B. Fornberg, V. Bayona, and G. A. Barnett. On the role of polynomials in rbf-fd approximations: I. interpolation and accuracy. *J. Comput. Phys.*, 321:21–38, 2016.
- [15] N. Flyer and G. B. Wright. A radial basis function method for the shallow water equations on a sphere. *Proc. R. Soc. A.*, 465(2106):1949–1976, 2009.
- [16] E. J. Fuselier and G. B. Wright. Stability and error estimates for vector field interpolation and decomposition on the sphere with rbfs. *SIAM J. Numer. Anal.*, 47:3213–3239, 2009.
- [17] E. J. Fuselier and G. B. Wright. A high-order kernel method for diffusion and reaction-diffusion equations on surfaces. *J. Sci. Comput.*, 56(3):535–565, 2013.
- [18] A. Gillette, M. Holst, and Y. Zhu. Finite element exterior calculus for evolution problems. *J. Comp. Math.*, 35(2):187–212, 2017.
- [19] J. B. Greer. An improvement of a recent eulerian method for solving pdes on general geometries. *J. Sci. Comput.*, 29(3):321–352, 2006.
- [20] B. J. Gross, N. Trask, P. Kuberry, and P. J. Atzberger. Meshfree methods on manifolds for hydrodynamic flows on curved surfaces: A Generalized Moving Least-Squares (GMLS) approach. *J. Comput. Phys.*, 409:109340, 2020.
- [21] S. Gross, T. Jankuhn, M. A. Olshanskii, and A. Reusken. A trace finite element method for vector-laplacians on surfaces. *SIAM J. Numer. Anal.*, 56(4):2406–2429, 2018.
- [22] J. Harlim, S. W. Jiang, and J. W. Peoples. Radial basis approximation of tensor fields on manifolds: from operator estimation to manifold learning. *J. Mach. Learn. Res.*, 24(345):1–85, 2023.
- [23] E. Hermans, M. S. Bhamla, P. Kao, G. G. Fuller, and J. Vermant. Lung surfactants and different contributions to thin film stability. *Soft matter*, 11(41):8048–8057, 2015.
- [24] A. N. Hirani. *Discrete exterior calculus*, Ph.D. thesis. California Institute of Technology, 2003.
- [25] M. Holst and A. Stern. Geometric variational crimes: Hilbert complexes, finite element exterior calculus, and problems on hypersurfaces. *Found. Comput. Math.*, 12:263–293, 2012.
- [26] S. W. Jiang, R. Li, Q. Yan, and J. Harlim. Generalized finite difference method on unknown manifolds. *J. Comput. Phys.*, 502:112812, 2024.
- [27] A. M. Jones, P. A. Bosler, P. A. Kuberry, and G. B. Wright. Generalized moving least squares vs. radial basis function finite difference methods for approximating surface derivatives. *Comput. Math. Appl.*, 147:1–13, 2023.
- [28] E. J. Kansa. Multiquadrics—a scattered data approximation scheme with applications to computational fluid-dynamics—ii solutions to parabolic, hyperbolic and elliptic partial differential equations. *Comput. Math. Appl.*, 19(8-9):147–161, 1990.
- [29] J. Kim and P. Moin. Application of a fractional-step method to incompressible navier-stokes equations. *J. Comput. Phys.*, 59(2):308–323, 1985.
- [30] J. M. Lee. *Introduction to Riemannian manifolds*. Springer, 2018.

- [31] E. Lehto, V. Shankar, and G. B. Wright. A radial basis function (rbf) compact finite difference (fd) scheme for reaction-diffusion equations on surfaces. *SIAM J. Sci. Comput.*, 39(5):A2129–A2151, 2017.
- [32] D. Levin. The approximation power of moving least-squares. *Math. Comput.*, 67(224):1517–1531, 1998.
- [33] J. Liang and H.-K. Zhao. Solving partial differential equations on point clouds. *SIAM J. Sci. Comput.*, 35(3):A1461–A1486, 2013.
- [34] W.-K. Liu, S. Li, and T. Belytschko. Moving least-square reproducing kernel methods (i) methodology and convergence. *Comput. Methods Appl. Mech. Eng.*, 143(1-2):113–154, 1997.
- [35] V. Martin, J. Jaffré, and J. E. Roberts. Modeling fractures and barriers as interfaces for flow in porous media. *SIAM J. Sci. Comput.*, 26(5):1667–1691, 2005.
- [36] D. Mirzaei. Error bounds for gmls derivatives approximations of sobolev functions. *J. Comput. Appl. Math.*, 294:93–101, 2016.
- [37] D. Mirzaei, R. Schaback, and M. Dehghan. On generalized moving least squares and diffuse derivatives. *IMA J. Numer. Anal.*, 32(3):983–1000, 2012.
- [38] G. Monge. *Application de l'analyse à la géométrie à l'usage de l'Ecole impériale polytechnique*. Veuve Bernard, 1809.
- [39] S. Morita. *Geometry of differential forms*. Number 201. American Mathematical Soc., 2001.
- [40] B. Nayroles, G. Touzot, and P. Villon. Generalizing the finite element method: diffuse approximation and diffuse elements. *Comput. Mech.*, 10(5):307–318, 1992.
- [41] A. Petras, L. Ling, and S. J. Ruuth. An rbf-fd closest point method for solving pdes on surfaces. *J. Comput. Phys.*, 370:43–57, 2018.
- [42] C. Piret. The orthogonal gradients method: A radial basis functions method for solving partial differential equations on arbitrary surfaces. *J. Comput. Phys.*, 231(14):4662–4675, 2012.
- [43] A. N. Pressley. *Elementary differential geometry*. Springer Science & Business Media, 2010.
- [44] J. D. Pryce. *Numerical Solution of Sturm-Liouville Problems*. Oxford University Press, 1993.
- [45] S. J. Ruuth and B. Merriman. A simple embedding method for solving partial differential equations on surfaces. *J. Comput. Phys.*, 227(3):1943–1961, 2008.
- [46] M. Samavaki and J. Tuomela. Navier–stokes equations on riemannian manifolds. *J. Geom. Phys.*, 148:103543, 2020.
- [47] R. I. Saye and J. A. Sethian. Multiscale modeling of membrane rearrangement, drainage, and rupture in evolving foams. *Science*, 340(6133):720–724, 2013.
- [48] U. Seifert. Configurations of fluid membranes and vesicles. *Adv. Phys.*, 46(1):13–137, 1997.
- [49] V. Shankar, G. B. Wright, R. M. Kirby, and A. L. Fogelson. A radial basis function (rbf)-finite difference (fd) method for diffusion and reaction–diffusion equations on surfaces. *J. Sci. Comput.*, 63(3):745–768, 2015.
- [50] A. Singer and H.-T. Wu. Vector diffusion maps and the connection laplacian. *Comm. Pure Appl. Math.*, 65(8):1067–1144, 2012.
- [51] J. Stam. Flows on surfaces of arbitrary topology. *ACM Transactions On Graphics (TOG)*, 22(3):724–731, 2003.
- [52] P. Suchde. A meshfree lagrangian method for flow on manifolds. *Int. J. Numer. Meth. Fluids.*, 93(6):1871–1894, 2021.
- [53] P. Suchde and J. Kuhnert. A meshfree generalized finite difference method for surface PDEs. *Comput. Math. Appl.*, 78(8):2789–2805, 2019.
- [54] P. Suchde and J. Kuhnert. A fully lagrangian meshfree framework for pdes on evolving surfaces. *J. Comput. Phys.*, 395:38–59, 2019.
- [55] M. Taylor. *Partial Differential Equations I: Basic Theory*, volume 115 of *Applied Mathematical Sciences*. Springer, New York, 2nd edition, 2011.
- [56] M. Taylor. *Partial Differential Equations III: Nonlinear Equations*, volume 117 of *Applied Mathematical Sciences*. Springer, New York, 2nd edition, 2011.
- [57] H. Tyagi, E. Vural, and P. Frossard. Tangent space estimation for smooth embeddings of riemannian manifolds. *Information and Inference: A Journal of the IMA*, 2(1):69–114, 2013.
- [58] H. Wendland. *Scattered Data Approximation*. Cambridge University Press, 2005.

- [59] J.-J. Xu and H.-K. Zhao. An eulerian formulation for solving partial differential equations along a moving interface. *J. Sci. Comput.*, 19(1):573–594, 2003.
- [60] Z. Zhang and H. Zha. Principal manifolds and nonlinear dimensionality reduction via tangent space alignment. *SIAM J. Sci. Comput.*, 26(1):313–338, 2004.